IEEE Access
Multidisciplinary | Rapid Review | Open Access Journal

Received 15 June 2022, accepted 10 August 2022, date of publication 18 August 2022, date of current version 26 August 2022.

Digital Object Identifier 10.1109/ACCESS.2022.3199739

SURVEY

Recent Developments of Butler Matrix From Components Design Evolution to System Integration for 5G Beamforming Applications: A Survey

ABDULKADIR BELLO SHALLAH[1,2], (Member, IEEE), FARID ZUBIR[1], (Member, IEEE), MOHAMAD KAMAL A. RAHIM[1], (Senior Member, IEEE), HUDA A. MAJID[3], (Member, IEEE), USMAN ULLAH SHEIKH[1], (Senior Member, IEEE), NOOR ASNIZA MURAD[1], (Senior Member, IEEE), AND ZUBAIDA YUSOFF[4], (Senior Member, IEEE)

[1]School of Electrical Engineering, Faculty of Engineering, Universiti Teknologi Malaysia, Johor Bahru 81310, Malaysia
[2]Department of Electrical and Electronics Engineering, Kebbi State University of Science and Technology, P.M.B 1144, Aliero, Nigeria
[3]Fakulti Teknologi Kejuruteraan (FTK), Hab Pendidikan Tinggi Pagoh, Universiti Tun Hussein Onn Malaysia, Parit Raja, Johor 84600, Malaysia
[4]Faculty of Engineering, Multimedia University, Persiaran Multimedia, Cyberjaya, Selangor 63100, Malaysia

Corresponding authors: Abdulkadir Bello Shallah (shallah@graduate.utm.my), Farid Zubir (faridzubir@utm.my), and Zubaida Yusoff (zubaida@mmu.edu.my)

This work was supported in part by Universiti Teknologi Malaysia (UTM) under UTM Encouragement Research Grant 20J65, and in part by UTMShine Batch No. 5 under Grant 09G97.

ABSTRACT Beamforming networks for multiple beam antennas are believed to be in the vanguard of technological developments in mmWave for 5G wireless applications. The basic idea of beamforming technique is the application of multiple antenna elements radiating the same signal at an identical phase and wavelength, into one strong signal pointed to a specific direction. For low cost and power consumption, radio frequency beamforming networks (RF-BFNs) such as Blass matrices, Butler matrices, and Nolen matrices will play a critical role in achieving the ever-increasing demands in wireless technology. Therefore, this study aims to present a comprehensive survey and developments of RF-BFNs with (particular focus in Butler matrices). From the fundamental perspectives of the beamforming techniques and progress over time, component evolution includes branch-line coupler (BLC), Phase shifter (PS), and Crossovers to complete system Butler matrix (BM) integration. Different design techniques to improve bandwidth, size reduction, multi-band, and other performance characteristics are discussed extensively. Furthermore, the paper also discusses different geometry of Butler matrices in open microstrip transmission lines, substrate integrated waveguide (SIW) and gap waveguide (GWG) technologies highlighting key developments and research challenges from single band to dual-band operations. We expect this paper to provide more profound insights into the designs processes and suggest suitable ways to facilitate further developments of RF-beamforming networks at mmWave and sub-mmWave frequency ranges.

INDEX TERMS Beamforming networks (BFNs), Butler matrix (BM), fifth-generation (5G), metamaterial (MTM), millimetre-waves (mmWave), substrate integrated waveguide (SIW), gap waveguide (GWG), ridge gap waveguide (RGW), groove gap waveguide (GGW).

I. INTRODUCTION

The increase in global data traffic is compelling and expected to thrive for several years to come with the massive developments of intelligent vehicles, Internet-of-things, and other 5G wireless devices [1]. The high-frequency band (mmWave) is envisioned to be the frequency range with which these devices operate. The main benefit of these 5G networks is that they will provide greater bandwidth, high data rates (10 Gb/s), low latency, and low power

The associate editor coordinating the review of this manuscript and approving it for publication was Santi C. Pavone.

consumption [2]. There are two categories of 5G networks: mid-band (less than 6 GHz) sub-6 GHz 5G and millimeter-wave 5G that covers (30 GHz to 300 GHz) [3]. Phased array antennas are vital in 5G wireless and mobile communications to compensate for propagation loss [4]. One of the essential tasks in phased array design is the critical design of beamforming network (BFN) [5], [6]. Antenna beam steering and antenna beamforming are exciting techniques widely used in communications systems, particularly in 5G and other wireless technologies. The basic idea of beamforming technique is the optimal transmission/reception of the signal over different antennas or from different antennas by appropriately varying the signal amplitudes and phases to form a fixed directed beam towards the intended user and reducing the other signal interference. Whereas in beam steering, the required beam pattern can be dynamically controlled by altering the signal phases and amplitudes in real-time without changing the position of the radiating elements [7]. Nowadays, BFNs for beam-steerable antennas attract substantial attention due to their outstanding accuracy, connectivity, and massive spectrum efficiency [8]. A conceptual diagram of a basic phase array antenna, beamforming, and beam steering techniques are shown in Fig. 1.

BFNs are generally classified into three categories, digital beamforming networks (D-BFNs) [9], analogue beamforming network (A-BFNs) [10], and hybrid beamforming networks (H-BFNs) [11]. In contrast, digital beamforming such as multiple-input-multiple-output (MIMO) proves to be one of the most widely used approaches for generating individual steerable multiple beams because of its flexibility [9], [12], [13]. However, high power consumption, hardware cost, and analogue-to-digital offset errors continue to be preventive factors for its use in large-scale, low-cost applications. To realize the trade-off between hardware cost, complexity and system performance, H-BFNs, which is a combination of an analogue-digital network, may serve as an alternative option [14]. However, A-BFNs or RF-type beamforming networks provide a cost-effective, energy-efficient, and most widely used solution well-fitting into microwave systems because of their simplicity.

The RF-BFNs, in contrast, are further grouped into two sub-categories that include quasi-optical (Rotman lens) [15], [16], and RF-based BFNs [5]. The former is a true time delay (TTD) device suitable for uttermost wide-band operations, making it a trending BFN due to its simplicity, reliability, and higher millimetre-wave frequency applications. At the same time, the most commonly known RF-based beamforming networks are Blass [17], Nolen [18], and Butler Matrix (BM) [19].

The 5G mobile network presents New Radio (NR) as a new air interface standard. This concept will enlarge cellular networks beyond mobile devices and conventional cellphones due to higher data rates and low latency attributed to the 5G network. Thus, it made it significant for new frequency allocations. The 5G NR frequency spectrum bands are classified into two different ranges. The first frequency range 1 (FR1) includes the bands used currently by previous generations and a new band in the sub-6 GHz range. Whereas the other frequency range (FR2) covers the higher frequency bands in the mmWave range spanning from (24 GHz to 100 GHz). The new frequency spectrums provide broader bandwidths allowing the application of internet-of-things (IoT), augmented reality (AR), and machine to machine (M2M) communications. Therefore, 5G provides new challenges for BFNs that must be compact, highly integrated, wide-band, and or multi-band designed at FR1 and FR2 frequency ranges.

Consequently, this paper provides an extensive review of analog type beamforming networks with particular focus on Butler Matrix designs. Different design techniques in open microstrip transmission line, substrate integrated waveguide (SIW), and low loss gap waveguide (GWG) technology are presented. State-of-the-art progress is reported, methods to improve performance such as compactness, widening bandwidth, dual-band, insertion loss, and phase deviation are discussed. To the best of our knowledge, this is the first extensive survey of Butler matrix based beamforming networks covering various design approaches from open microstrip transmission line, SIW and the low loss GWG technologies. We believe that this review paper will give the needed impacts and provide future perspectives in developing beamforming networks for mmWave and sub-mmWave applications.

The remaining of this paper is organized as follows. Section II provides a fundamental theory of RF-BFNs, and it discusses the general background and concept of beamforming classified based on their feeding techniques. Apparent similarities, advantages, and disadvantages of each class over another are also discussed extensively.

Section III discusses the essential components of the Butler matrix that include branch-line coupler (BLC), phase shifters (PS), and crossover (CO) are presented. The latest development on size miniaturization, wideband, and dual-band enable techniques will be thoroughly discussed. Subsequently, section IV presents a detailed discussion of different innovative methods and performance improvement techniques of several BM designs focusing on compactness, bandwidth enhancement, and multi-band operation while maintaining other performance parameters within the acceptable range. Finally conclusion and future direction are presented in section V.

II. FUNDAMENTAL THEORY OF RF-BFNs

A. GENERAL CONCEPT

When fed by an input signal, A-BFNs generate several simultaneous signals from the same physical layer of an array antenna having both amplitudes and phases responses needed to direct its beam in the required direction in space. These networks have an equal number of input ports M, connected to output ports N with both M and N as integers, and the networks are often described as $M \times N$ devices. The power at the input ports is expected to be fully transferred to the output ports. In transmitting mode, BFNs are characterized by their

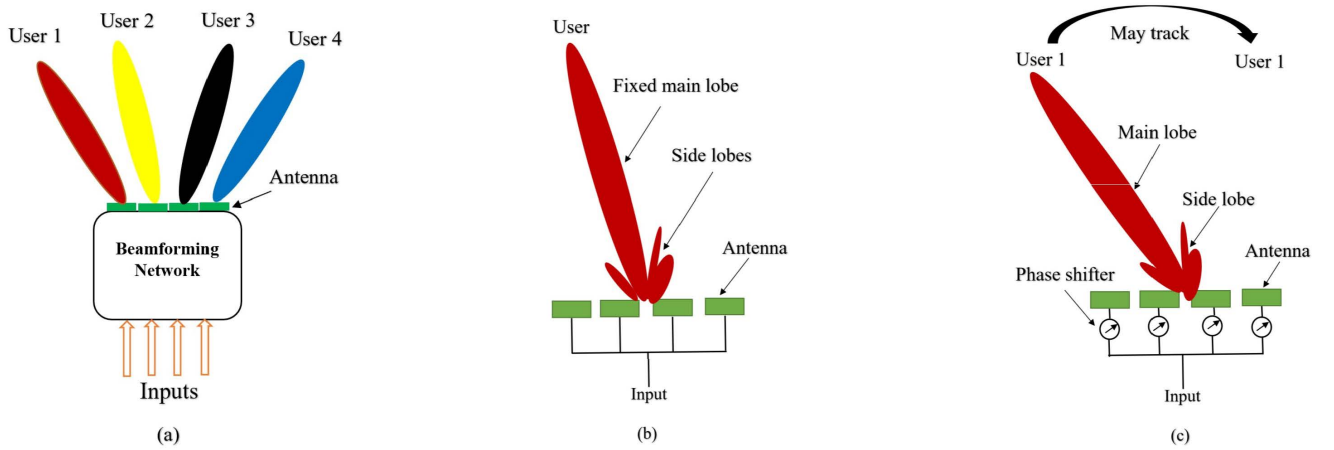

FIGURE 1. Basic diagrams. (a) Phase array antenna. (b) Beamforming technique. (c) Beam steering technique.

transfer matrix S. The excitation coefficient vector X_i where i is the matrix column elements produced by exciting the beam port i, which varies from $1 \ldots M$, while the elements Y_j $j = 1 \ldots N$ of the y corresponds to the vector delivered at the array elements (output port). Theoretically, lossless beamforming should provide orthogonal excitations in the radiating elements resulting in orthogonal beam patterns in space under the assumption that the remaining scattering parameters of the matrix are negligible when all ports are matched and decoupled [20]. Thus, a single aperture can produce multiple autonomous radiation beams sequentially when BFN input ports are fed. At the same time, all corresponding beams are simultaneously available on receive mode.

Furthermore, circuit-based BFNs can also be classified based on their feeding topology: series feeds (Blass and Nolen matrices) and parallel feeds (Butler matrix).

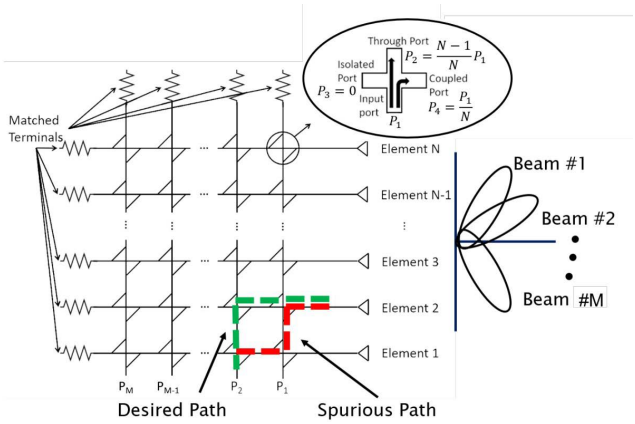

FIGURE 2. Blass matrix schematic diagram [26].

B. SERIES FEED TOPOLOGY

The basic building blocks of RF-based BFNs are phase shifters, directional couplers, and crossovers. When a wireless signal with identical phases and amplitudes is fed at the input, a simultaneous radiation pattern is produced by the whole array pointing in particular directions.

The Blass matrix was first introduced in the early 60s [21]. It consists of N number of rows and M number of columns; N corresponds to the number of beams simultaneously produced while M is connected to the antenna elements as feeder lines. It is composed of only couplers and phase shifters with no crossovers but rather load terminations at each line end. The two transmission lines are interconnected at each crossover by a directional coupler. The input signal applied at each port propagates along the feed lines that are terminated by the matched load to prevent reflections. The significant advantage of the Blass matrix is its flexibility with great potentiality to generate multiple beams positioned to point in arbitrary directions. However, the performance of the Blass matrix is hindered by losses and makes it challenging to design due to the presence of matched loads and interaction between the feeding lines and those placed above them as illustrated in Fig. 2. Therefore, very few efforts were made on Blass matrix design [17], [22], [23], [24], [25], [26].

Another BFN according to series feed topology is Nolen Matrix [27], that consists of a four-port coupler and phase shifters. The amplitude coupling coefficient of the coupler is determined by the progressive weight of θ, as illustrated in Fig 3. It was first introduced in 1965 [28] as a lossless form of Blass matrix whereby simple bends are used in place of the couplers at the diagonal connecting two successive ports. The couplers after the diagonal are removed since they are no longer linked to the inputs or outputs ports. Similarly, from the reported works [18], [29], [30], [31], one can easily see a comparison with its Butler matrix counterpart in complexity for planar realization. So basically, the Nolen matrix can be regarded as a hardware form of discrete fourier transform (DFT) that can be reduced to a more straightforward form and applied to any number of output ports. Just like fast fourier transform (FFT) analogue equivalent BM that will be discussed next section [32], [33].

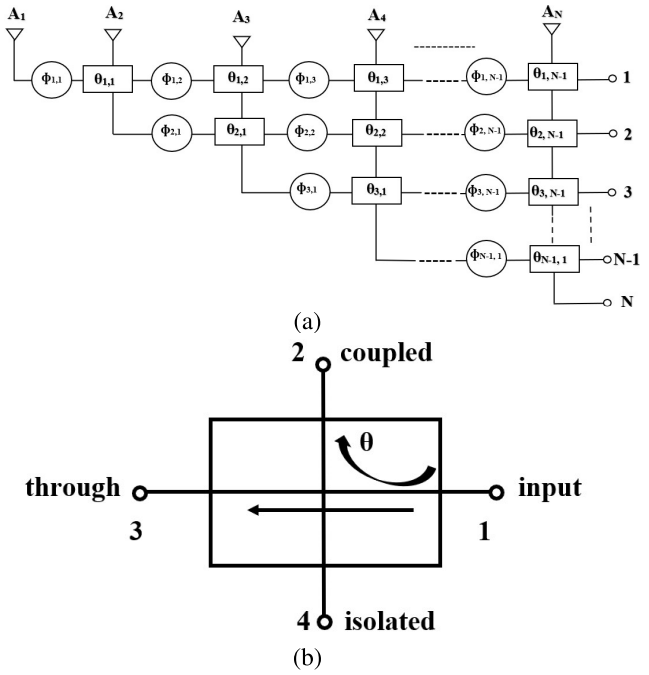

FIGURE 3. (a) General layout of Nolen matrix and (b) Coupler at the node [29].

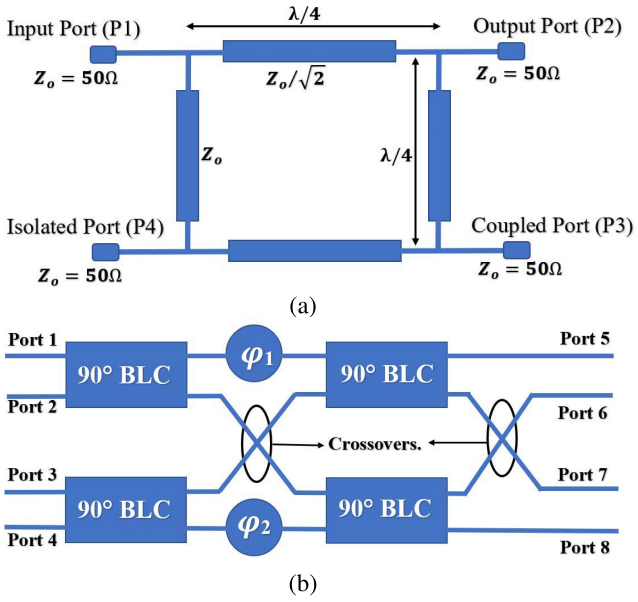

FIGURE 4. Schematic diagram. (a) 3 dB Branch-line coupler. (b) 4 × 4 Butler matrix.

C. PARALLEL FEED TOPOLOGY

Butler matrix is a passive BFN for feeding multi-beam antenna characterized by parallel feed topology. This BFN, first introduced in [33], consists of N number of input ports (the beam ports) connected to transceiver and N equal number of output ports (the elements ports) connected to the array elements. The port number N is an positive integer with the power of 2, $N = 2^n$, with n also an integer. A signal applied in any input port generates equal amplitudes with progressive phase differences excitations, resulting in a beam pointed in a particular direction. Thus, the beam direction in space is determined by applying a signal through a specific input port. The essential components of Butler matrix BFN are characterized by $(N/2 \times log_2 N)$ the branch-line coupler, phase shifter, and 0 dB crossovers. Due to its simple structure, the most widely used BM is 4 × 4, as depicted in Fig. 4(b). It consists of four 3 dB couplers, two 0 dB crossovers, and two 45° phase shifters, with ports 1 to 4 as excitation ports (beam ports) and ports 5 to 8 as output ports (array ports) respectively [34]. All ports are isolated and matched to the network impedance [35]. Fig. 4(a) illustrates a Quadrature branch-line coupler (QBLC). It consists of two input and output ports with a 90° phase delay between the output ports. The QBLC is implemented using two vertical and horizontal transmission lines of $\lambda/4$ length each; the characteristic impedance of the lines is Z_o and $Z_o/\sqrt{2}$ respectively. When the signal is fed into port 1, it separates it into two equal parts with equal amplitude and 90° phase shift between them. Port 1 as an input port, port 2 and 3 output and coupled port respectively, while port 4 is terminated at 50 ohms and isolated from the input port. The crossover is made by cascading two 90° BLC. The function of the crossovers is to create a path for signal into the second stage with high isolation and 0 dB insertion-loss [32]. The effect of connecting two BLC in cascade will add 90° phase shift to the lines being crossed, which can be balanced by attaching an equivalent amount to the phase shifters in the uncrossed lines. Ideally, theoretically, BLC crossover has zero couplings between the two paths [36]. Therefore, the phase shifters required in this kind of implementation are constructed as delay lines of appropriate length determined by $L = (\phi \times \lambda)/2\pi$, where ϕ is the required phase shift [34].

Table 1 presents the advantages and disadvantages of each type of beamforming network.

III. CONSTITUENT OF BUTLER MATRIX

Butler matrix, as described earlier, consists of three primary devices; these devices include quadrature coupler, phase shifter, and crossovers. Careful design and proper synthesis of every device within the circuit result in an excellent BM circuit according to desired applications. In this section, the latest developments of such devices as presented by several researchers are discussed.

A. BRANCH-LINE COUPLER (BLC)

The BLC otherwise known as quadrature coupler, is an essential circuit element that constitutes the Butler matrix among these devices. Conventionally, BLC is built using four $\lambda/4$ wavelength transmission lines of 50 ohms (vertical arm) and $50/\sqrt{2}$ Ohms (horizontal arm) characteristics impedances sections each. BLCs are 3 dB devices with a 90° phase difference from the two outputs ports termed the coupled and through ports, which usually limits the coupler

TABLE 1. Advantages and disadvantages of analogue beamforming networks.

	Blass matrix	Nolen matrix	Butler matrix
Advantages	✓ It has no crossovers. ✓ The number of input and output ports may not necessary be equal. ✓ Ability to provide multiple beams directed in arbitrary positions. ✓ Highly flexible. ✓ Low manufacturing cost.	✓ It is technically lossless. ✓ Ability to provide wide frequency bandwidth. ✓ Low fabrication cost. ✓ Less complex structure.	✓ It has fewer number of components. ✓ Theoretically lossless. ✓ Compact and simple structure. ✓ Low fabrication cost. ✓ No external control. ✓ Suitable input impedance and port isolations.
Disadvantages	✗ It is lossy due to load terminations. ✗ Interaction between feeding lines. ✗ Low flexibility for coupler design. ✗ Limited bandwidth.	✗ Coupler design limitations. ✗ Interactions between feeding lines. ✗ Frequency dependant beams.	✗ Beam directions are pre-defined. ✗ Complex structure for larger networks. ✗ Port numbers has to be symmetrical with power of two. ✗ Pre-determined output phases.

operation within a single band operation. Moreover, this device's compact size and good performance are often stringent expectations in BM design systems. The geometry of the typical BLC structure is illustrated in Fig. 4(a). The equivalent even and odd modes' analyses are usually employed in BLC analysis. ABCD parameter matrices are used to evaluate the circuit's overall transmission and reflection characteristics.

Even mode:

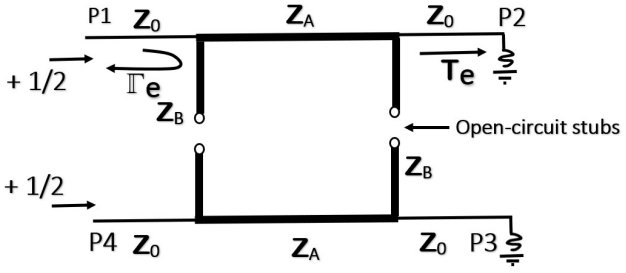

$$\begin{bmatrix} A & B \\ C & D \end{bmatrix} = \begin{bmatrix} 1 & 0 \\ jY_B & 1 \end{bmatrix} \begin{bmatrix} 0 & jZ_A \\ jY_A & 0 \end{bmatrix} \begin{bmatrix} 1 & 0 \\ jY_B & 1 \end{bmatrix} \quad (1)$$

$$\Gamma_e(S_{11}) = \frac{A+B-C-D}{A+B+C+D} = 0 \quad (2)$$

$$T_e(S_{21}) = \frac{2}{A+B+C+D} = -\frac{(1+j)}{\sqrt{2}} \quad (3)$$

Odd mode:

$$\begin{bmatrix} A & B \\ C & D \end{bmatrix} = \begin{bmatrix} 1 & 0 \\ -jY_B & 1 \end{bmatrix} \begin{bmatrix} 0 & jZ_A \\ jY_A & 0 \end{bmatrix} \begin{bmatrix} 1 & 0 \\ -jY_B & 1 \end{bmatrix} \quad (4)$$

$$\Gamma_o(S_{11}) = \frac{A+B-C-D}{A+B+C+D} = 0 \quad (5)$$

$$T_o(S_{21}) = \frac{2}{A+B+C+D} = -\frac{(1-j)}{\sqrt{2}} \quad (6)$$

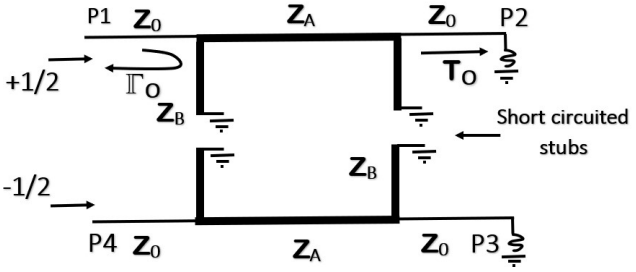

Having characteristic admittance of the conventional branch-line coupler $Y_A = \frac{1}{Z_A} = \sqrt{2}$ and $Y_B = \frac{1}{Z_B} = 1$, where T_e, Γ_e and T_o, Γ_o represents transmission and reflection coefficients of the even and odd modes respectively.

Therefore, for an ideal matching condition: the scattering parameter matrix of the standard BLC is:

$$[S] = \begin{bmatrix} S_{11} & S_{12} & S_{13} & S_{14} \\ S_{21} & S_{22} & S_{23} & S_{24} \\ S_{31} & S_{32} & S_{33} & S_{34} \\ S_{41} & S_{42} & S_{43} & S_{44} \end{bmatrix} = \frac{1}{\sqrt{2}} \begin{bmatrix} 0 & j & 1 & 0 \\ j & 0 & 0 & 1 \\ 1 & 0 & 0 & j \\ 0 & 1 & j & 0 \end{bmatrix} \quad (7)$$

The matrix above shows that the branch-line coupler is symmetrical and equally splits the power fed through either input port into two with an equal amplitude but 90° phase difference between the output ports. The fourth port completely isolated, and there is zero power reflection back at the input port. Hence, the directivity and isolation of the matched coupler are very high at the operating frequency. Therefore, the BLC's compactness, wide-band, and multi-band operation influence many microwave communication systems' performances. To achieve these functions, the $\lambda/4$ wavelength transmission lines of the conventional couplers are usually converted into their equivalent circuits according to the specific design and operations. It can be obtained by equating the ABCD matrix of the traditional transmission

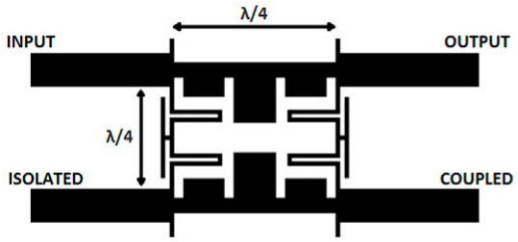

FIGURE 5. Proposed U and T shaped BLC [39].

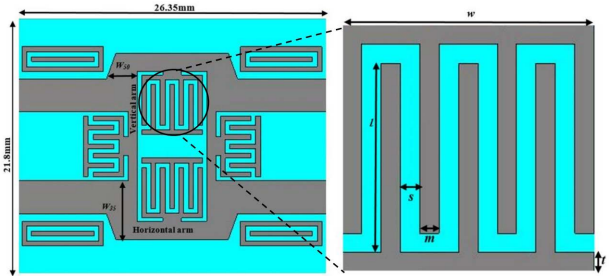

FIGURE 6. Layout of the proposed BLC [44].

line's ABCD matrix to the desired coupler design [37]. For the conventional transmission line section in Fig. 4(a), the ABCD matrix is given by:

$$\begin{bmatrix} A & B \\ C & D \end{bmatrix}_{\frac{\lambda}{4}} = \begin{bmatrix} \cos\theta & jZ\sin\theta \\ \frac{j}{Z_o} & \cos\theta \end{bmatrix} \begin{bmatrix} 0 & jZ_o \\ \frac{j}{Z_o} & 0 \end{bmatrix} \tag{8}$$

Over the past years, several methods have been investigated for size reduction, bandwidth enlargement, wide-band, and multi-band operations and reported in the literature.

1) SINGLE-BAND BLC

Das *et al.* [38] proposed a folded microstrip TL section as a miniaturization technique for compact BLC design. The method is fast and achieved excellent performance with a 43.63% size reduction at a 3 GHz frequency. However, the bends introduced in the design resulted in a shift of center frequency and required a high optimization level. A miniaturized BLC for LTE application is proposed in [39]. In this article, the conventional $\lambda/4$ TLs were replaced by U and T-shaped TL sections, as illustrated in Fig. 5. The design is compact and covers a dimension of 50 $mm \times 19.51$ mm at 2.2 GHz center frequency.

In [40], a novel miniaturized 3-dB coupler using a stepped impedance resonator was proposed. For size reduction, Π and T-model TLs were employed to replace conventional quarter-wave transmission lines with a 20 $mm \times 25$ mm dimension, which is about 50% size reduction compared to traditional design at 2.45 GHz frequency operation. A compact cascaded coupler using T-sections was proposed in [41] to achieve wide-band operation. In this design, cascaded sections were used to enhance the bandwidth, which increased coupler size due to the nature of the coupler. Hence T-shaped was employed to further miniaturize the structure. The method provides 34.4% bandwidth with a 66.5% size reduction at 3 GHz center frequency. Artificial transmission lines (ATL) replaced the conventional TL to achieve compactness [42]. The authors considered a high resistance open stub and a U-form high resistance segment for miniaturization of the devices. The former achieved a 76% size reduction, while the latter produced a 69.1% size reduction compared to the standard design. However, the bandwidth usually tends to be smaller than the traditional design due to the shift of frequency caused by discontinuities in the structure. Hence cascaded sections were employed to enhance the bandwidth.

To realize wideband BLC, a three section coupler designed using triple complementary split ring resonator (CSRR) and open stubs cascaded together is presented [43]. The CSRR employed provides 82.56% size reduction compared to the conventional method and provide 53% useful bandwidth.

A novel miniaturized BLC based on complementary right/left hand TL was reported in [44]. The inter-digital structure and double spiral defected resonance cell provided the needed impression of the negative permittivity and permeability. Hence, the design used the composite right/left handed transmission line (CRLH-TL) structure instead of conventional TL. The structure achieved a 66% size reduction over a 1 GHz center frequency. Interdigital capacitor structure was also used to miniaturize the BLC in [45]. Moreover, open-circuit coupled lines were placed parallel with the port lines to improve the bandwidth further, as shown in figure 6. The design demonstrates an excellent performance with 54% size reduction and achieved 40.2% fractional bandwidth over 2.74 – 4.15 GHz frequency band.

In summary, the conventional BLCs typically occupy large circuit areas due to their quarter-wave transmission lines sections. This, however, further narrow the operational bandwidth, especially at high-frequency bands. The bandwidth enhancement of the BLCs was mainly achieved by cascading two or more transmission line sections as reported in [41] and [42]. But the circuit size increased compared to the conventional BLC. Since then, researchers have adopted several ways of innovative coupler implementations, focusing on compactness, low cost, and ease of fabrications. Different design methods to improve bandwidth have been reported in the literature such as open-circuited series stubs, dual quarter-wave transformer, unequal power division ratio, and placing open-circuit coupled lines parallel with the port lines as reported in [45]. To this end, it is understood that due to the limited bandwidth of the conventional couplers, their application in wide-band and multi-band systems is limited to single frequency band operations. The advancement of multi-band communication systems demands the innovative design of multi-band BLCs. Latest developments from the available literature to enable dual-band operations in the following subsection.

2) DUALBAND BLC

Dual-band BLC display certain functionality at two different frequency bands. The most convenient method to obtain a

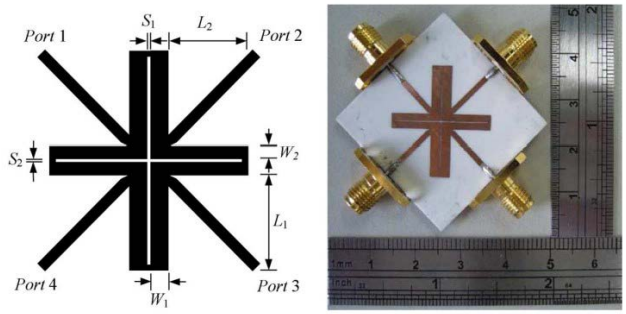

FIGURE 7. Structure of the dual-band BLC [48].

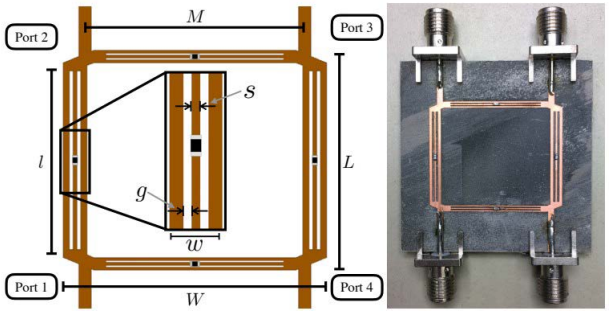

FIGURE 8. Structure of the MTM-EBG dual-band BLC [56].

dualband operation for BLC is to transform the components of a single band coupler into its dual-band counterpart. Open or short stubs seem to be a suitable option due to their reactive properties; thus can help obtain multiple frequency responses in a single device. Therefore, various techniques have been reported to produce multi-band operations in a coupler.

A novel approach to designing and implementing a dual-band compact coupler is proposed in [46]. In this method, the quarter-wavelength branches are converted to Π-mode by attaching stubs at the two ends of the branches evaluated at the mid-frequency of the two desired bands. However, the added stubs enlarged the circuit, and the design is restricted by the range of impedances that can be realized; thus, dual-band frequency ratios are also limited. To achieve a more compact layout and improve frequency ratio, Π-mode step impedance stubs with reduced electrical length coupler were reported [47]. Another design method to obtain more compact and dual-band operation is by substituting coupled lines in place of the conventional transmission line branches as demonstrated in [48]. As shown in Fig. 7, the structure was designed to have unequal output power at the two frequency bands.

A dual-band coupler with attached open-ended and short-ended cross-shaped stubs was introduced in [49]. The structure is compact with a wide frequency ratio and operates at 1 GHz and 3.5 GHz frequency bands. Another design method to obtain a wide frequency ratio is using a couple-line with attached open stubs as demonstrated in [50]. The coupled line provides the dual-band operation in the design while employing opened stubs of different characteristic impedance values further enhances the frequency ratio operation. A planar dualband BLC with a large frequency ratio was proposed in [51]. This design used an E-shaped BLC from two cascaded Π -shaped open and short stubs to demonstrate two prototype couplers for 1/8 GHz and 2.4/5.2 GHz frequency bands showing excellent performance characteristics.

The dual-band BLCs designed using open and short stubs require more space than the single-band microstrip designs, making the device bulky and more complex to fabricate. Another design method to develop a compact dual-band BLC is to employ the metamaterial (MTM) technique. This technology provides unusual characteristics that cannot be found naturally, such as negative phase constants. The reactance of a conventional transmission line in the positive region can now be effectively controlled in the negative region. A novel compact dualband BLC utilizing CSRR with coupled line technique was proposed in [52]. The structure demonstrate high degree of miniaturization with a 90% size reduction compared to some previous designs. The work in [53] proposed a novel structure that acts as dual-band BLC at lower frequency band of 3.3 and 3.85 GHz and acts as a 180° rat-race coupler at a higher frequency band of 5.3 GHz. the novel structure is implemented using open split ring resonators based ATL.

In [54] and [55], the design demonstrates that traditional TLs, characterized by the distributed series inductance and shunt capacitance, can be made much smaller by adding lumped-type reactance periodically in a unit cell, composite right/left hand transmission line (CRLH-TL) can be constructed. MTM-EBG based on a microstrip medium can also allow the dual operating frequencies as reported in [56]. As shown in Fig. 8, the structure has a series loading capacitor in the coplanar waveguide strip conductor placed in the branches of a BLC. It enables the device to support a second operating frequency relatively close to the other. In [57], a dualband coupler based on CRLH-TL is utilized to implement a dual-band balun to operate at 2.4 and 3.5 GHz frequency bands. The designed structure is compact with about 20 mm^2 dimensions.

To this end, various techniques have been proposed to make the BLC operate in dual frequency bands. The most common method is to attach stubs of required impedance to the uniform transmission line. However, these often cause the structure to be much bigger, occupying a larger area than the corresponding single-band designs. Moreover, some researchers proposed that the stubs be arranged within the four corners of the BLC to make it more compact. Similarly, these further make the design more complex and difficult to fabricate. The MTM approach is the most convenient technique to design a more compact dual-band coupler. Although resonance type structures such as split ring resonator (SRR), and CSRR can provide dual-band operations and significantly reduce size compared to traditional TL designs, they generally suffer from high loss and narrow bandwidth as described

in [58]. It was shown that MTM-EBG [56], CRLH-TL [54], [55], [57], can be used to realize a $\lambda/4$ length transmission lines with 90° phase difference at two frequency bands and exhibit broad bandwidth and low loss simultaneously.

B. MICROWAVE PHASE SHIFTERS (MPS)

A MPS is a device designed to change the phase of electromagnetic signals at the output of the microwave transmission line to a specified degree, with respect to the phase of the signal at the input. Phase shifters, just like BLCs, are widely used microwave devices in many microwave circuits and beamforming networks. Generally, phase shifters can be divided into two classes: analogue phase shifters that provide a continuous phase shift or delay line [58], [59], and digital phase shifters that provide a discrete set of phase shift or delay lines [60]. As a good performance, planar phase shifters featured compact size, simple design, and relatively wide bandwidth is required for practical applications. Traditionally, the Butler matrix's phase shifters are fixed and use delay lines to provide the required phase shift. However, the narrowband nature of this circuit significantly limits the operation bandwidth of the design.

The Schiffman device was the earliest planar circuit introduced in the late 50s [61]. It is a passive instrumental component and the most attractive differential phase shifter due to its simplicity and broadband characteristics [62]. It consists of two parallel-coupled lines of equal length with one side shortened and producing a delay of 90° over a specified bandwidth. However, it required a high degree of coupling that broadside coupled lines must be employed. Furthermore, the work was based on stripline structure, where both odd and even modes propagate with equal phase velocity. Contrary to the design in microstrip transmission form, where the phase velocity of odd and even modes are unequal, and thus the coupling ratio produced is limited. Therefore, this issue was acknowledged and several modifications have been reported to compensate for the discrepancy between the even and odd mode phase velocities. Like using a coupled line with a modified ground plane to increase the even-mode impedance as demonstrated in [63]. Similarly, the same modified ground structure was employed in [64] with a dentate microstrip transmission line for broadening the operational bandwidth. More recently, articles [65], [66] demonstrate that Schiffman phase shifters can also operate in their second phase period suitable for more considerable phase shift value greater than 90° and broader phase shift bandwidth using the same coupling coefficient. In addition to their operational bandwidth limitations, microwave phase shifters also suffer from large dimensions. Hence, the MTM approach has also been the key technique for developing a more compact phase shifter. In [67], a significant size reduction of the conventional phase shifter was achieved by employment CSRRs etched on the ground plane.

In order for phase shifters to operate over dual frequency bands simultaneously, conventional wideband phase shifters barely realize independent phase shift values in different frequency bands with good isolations. Therefore, developing dual-band phase shifters having two separate and constant phase shift bands is paramount. Even so, somewhat few techniques to obtain dual-band phase shifters have been reported. The work in [68] presents a reconfigurable circuit operating in two different phase shifts. Two reactive loads controlled by two single-pole-double-throw (SPDT) switches are employed to obtain the two different phase states. In [69] and [70], dual-band stub-loaded structures in the forms of Π-shape and T-shape that produced arbitrary phase shifts at two frequency bands have been demonstrated.

Moreover, to obtain simultaneous dual phase-shift in two independent frequency bands, coupled lines with attached shorted-circuited stubs at each end of the line were presented in [71]. As mentioned earlier, all the techniques primarily focused on achieving simultaneous phase shifts at different frequency bands. They are designed at two independent frequencies, hence suffer a limited phase shift bandwidth. Therefore, Dong *et al.* [72] and Qiu and Zhu [73], proposed synthetic methods to develop differential phase-shifters with first and second-order predetermine phase-shifting bands and independent filtering passbands. Similarly, CRLH-TLs have been applied for achieving dual-band PS in [74] and [75].

C. MICROWAVE CROSSOVER (CO)

Microwave crossovers are passive devices that allow microwave signals to pass across one another with relatively zero interference between them. In the design of microstrip circuits, transmission lines usually require crossings between two lines with high isolation purity. However, when two transmission lines overlap, the signal stability tends to be affected by the interfering signal between them, thus affecting the signal purity at the output port. Along with basic requirements in high-density microwave circuits, Co is one of the structural components used in Butler matrix design for beamforming applications [76]. Generally, the crossovers are realized using air bridges, underpasses, or multilayer substrates [77], [78]. The airbridge is implemented using microelectromechanical system (MEMS) processing and bond wires, increasing cost and occupying a large circuit area.

On the other hand, multilayer approaches are made where the transmitting signal passes between different layers and requires microstrip-coplanar waveguide-microstrip transitions. Vias and slot lines are also necessary, increasing complexity and fabrication difficulties. The most widely used planar crossover is based on the sections of microstrip transmission lines. The structure is achieved by cascading two BLCs providing a better operation bandwidth as described in [79]. However, the circuit dimensions are relatively large at low microwave frequencies when integrated to other systems. In order to attain a more compact crossover structure, the transmission lines were replaced by capacitive loaded ATL in [80] achieving size miniaturization of 30% less than the conventional design. In [81], the geometric size of the crossover was reduced by substituting the quarter-wave transmission line section with a low pass filter that retains the

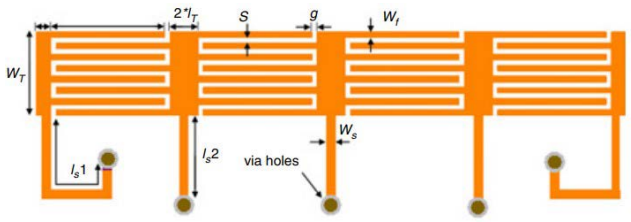

FIGURE 9. Proposed balanced-to-single ended crossover [90].

same phase shift as the replaced segment. The structure is compact with 64% reduced surface area compared to the standard design. Jayakrishnan *et al.* [82], [83] also demonstrated that crossover region can be made using a microstrip patch technology. Similarly, for crossover size-reduction, MTM structure can also be employed as presented in [84].

All the crossover designs mentioned above operate in a single frequency band only. For multi-band operation, individual components for microwave systems should be compact and cost-effective with considerably high-performance characteristics at different frequency bands. A planar dual-band crossover with asymmetrical Π-shaped TLs was developed in [85] and [86]. A compact dual-band crossover using symmetrical H-shaped structures is also reported [87]. Inspired by [85] and [86], the crossover miniaturization was achieved by reducing the number of inner open stubs in [88]. Derived from a standard patch structure, a cost-effective and straightforward dual-band crossover was proposed [89]. Another design method to develop a dual-band crossover is proposed in [90]. In this method, two CRLH-TLs that control frequency ratio were utilized to create a dual-band balanced structure, as illustrated in Fig. 9.

IV. MICROSTRIP TL BUTLER MATRIX

Traditionally, microstrip transmission lines are used to propagate microwave-frequency signals. It is one of the many forms of planar transmission line structures along with stripline and coplanar waveguide that can easily be integrated on the same substrate [91]. It is simple, low cost, and almost supports the transverse electromagnetic (TEM) propagation mode. It is lighter and more compact. However, microstrip TL suffers from low power handling capacity, high losses, and susceptibility to crosstalk and spurious radiation. Microstrip material has inherent bandwidth limitation from which TL is made up [92], [93].

Furthermore, Butler matrix consists of 90° BLC, 45° phase shifter, and 0 dB crossovers that can be easily constructed using microstrip owing to various advantages that include low profile, low cost, and easy fabrication. However, the conventional BLC, the primary building block of BM design, is based on four transmission lines of $\lambda/4$ length provides a narrow bandwidth. Similarly, the dimension is comparable to the wavelength hence considerably large [94]. Furthermore, the bandwidth of the multi-beam antenna array is primarily restricted by the BFNs instead of antenna elements [95]. Therefore, many research focused on BM performance improvements such as bandwidth enhancement, size miniaturizations, and multi-band systems of wireless communication devices operating across the frequency ranges of interest.

A. SINGLE BAND BUTLER MATRIX

The increasing use of 5G devices at a high-frequency range mmWave has become the day's subject in the wireless communication industry. Antennas for 5G applications usually utilize smaller element sizes at a high-frequency range. When designing a BM-based multi-beam antenna system, the area occupied by BM is generally much larger than the array elements themselves. Therefore, BM size reduction is more critical for the entire form factor minimization [96]. Crossovers have also been the significant bottleneck for BM structure for a long time. The traditional design is subject to limited bandwidth and large electrical size due to $\lambda/4$ length transmission-line sections [97]. To mitigate the problem, several techniques have been reported by many researchers, such as BM without crossovers [98], [99], [100], [101], [102], with transformed Branch line coupler [103], [104], BM with the introduction of MTM structure [105], [106], [107], [108], [109], [110], [111], [112], [113] and ATL-based BM [114], [115], [116], [117]. Some new concepts improved bandwidth whereas others achieved size reduction by removing crossing entirely.

In [97], a novel broadband quadrature coupler was introduced by combining patch coupler and coupled line. The patch coupler is a rectangular patch with two cross slots that creates two near resonances and a novel broadband phase shifter with changing length and width of the feed-line as shown in Fig. 10. The reported design operating at 35 GHz center frequency achieved wide bandwidth of about 3.95 GHz at the expense of having size and fabrication complexity. Four different 4×4 BM topologies operating at 2.44 GHz were designed in [98]. The design with the shorter TL length was used to fabricate an 8 × 8 BM structure at 1.9 GHz. However, the structure becomes more complex as more input and output ports are required. The network reported in [99] further affirmed what was earlier said in [98]. As the structure size increases, the output ports would be forced to be placed on the inner side of the structure while the input ports are placed on the outer side. That means the array elements will be placed at the center of the BM structure, and parasitic radiations of the BM will affect the antenna radiation, thus degrading the overall performance. The work in [100] proposed a 4 × 4 BM without crossing. The structure was obtained by employing BLC with open stub and phase shifters of 45° and 90° to realize miniaturization. The design was compact and achieved excellent performance with a 42.68% size reduction compared to the traditional BM.

In [101], the structure consists of two modified BLCs and two 90° BLCs without any phase shifter and crossover. The compactness is achieved by two modified BLCs designed in such a way to replace 90° BLCs and 45° phase shifters

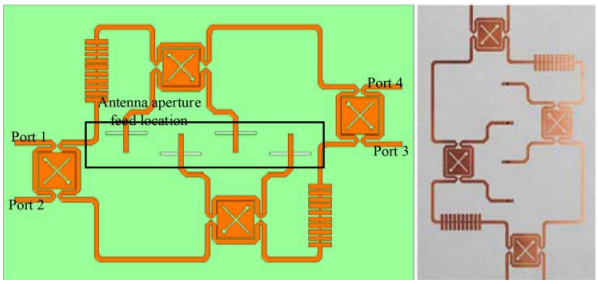

FIGURE 10. Structure of the broadband BM [97].

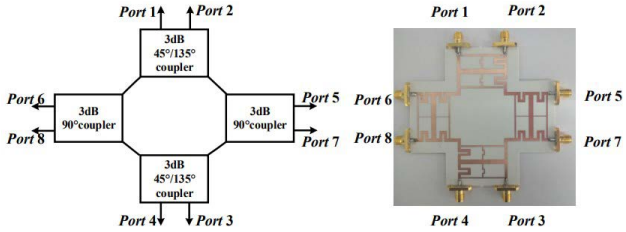

FIGURE 11. Layout of the designed 4 × 4 BM [104].

at 2 GHz frequency. A 4 × 4 BM with flexible phase difference without Phase shifters and crossover was proposed in [102]. The simulated result shows an excellent performance at 2 GHz operating frequency. Article [103] suggested a single layer 4 × 4 BM without phase shifter and crossover. A modified BLC replaced the phase shifter with a 45° phase difference achieving a 37.1% bandwidth at 6 GHz operating frequency. In [104], a wideband 4×4 BM constructed with a novel hybrid coupler with arbitrary phase difference was proposed. As illustrated in Fig. 11, the design achieved compactness by eliminating crossover and produced a wide bandwidth of 45.3% operating at 2.56 GHz.

A mesh quarter-wavelength microstrip TL loaded with CS-SRR in its ground plane was used to achieve 16.6% miniaturization in [105]. Another CSRRs based miniaturization technique ware reported in [106]. Phase delay characteristics of CSRR loaded in a ground plane were utilized to achieve 48% size reduction. The CSRRs were placed only at the phase delay length of the transmission line without offsetting the BLC and crossover. In [107], 4 × 4 BM was designed based on a perfect magnetic conductor. The proposed design is compact and has an excellent performance with enhanced bandwidth operating over the 27-31 GHz frequency range.

In [110], a wideband microstrip transmission line BM was designed and inverted over artificial magnetic conductor (AMC) realized by an array of mushroom-shaped electromagnetic band gap (EBG) unit cells. The purpose is to reduce the radiation loss due to discontinuities in the BFN. The design produced 30% bandwidth with a BM overall size of 60 *mm* × 50 *mm* at 30 GHz. The same authors adopted a similar concept in [109], where a single substrate microstrip transmission line 4 × 4 BM was incorporated within a perfect magnetic conductor (PMC) packaged environment to suppress losses, as shown in Fig. 12.

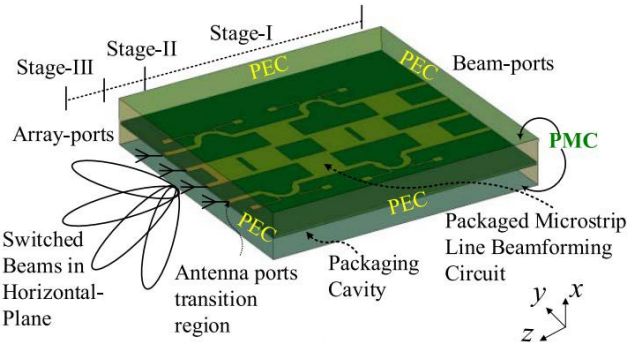

FIGURE 12. Layout of the shielded BM [109].

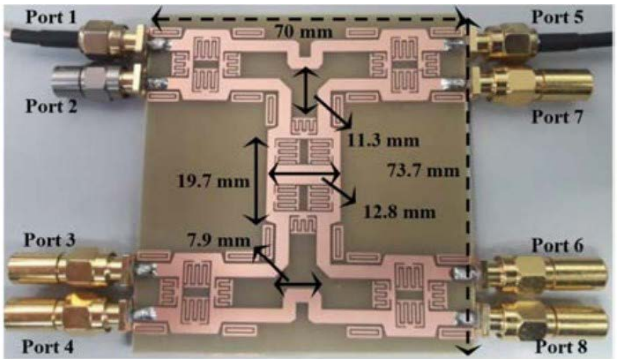

FIGURE 13. Fabricated compact 4 × 4 BM [112].

In [111], 4 × 4 square ring metasurface element array was used as a top layer to enhance scan angle of 2 × 2 BM fed antenna array operating at 28 GHz frequency. The system acquires about 3.4 GHz operating bandwidth. A 4 × 4 MTM-based BM was presented in [112]. The structure was made by incorporating open-circuit coupled lines and interdigital capacitor unit cells for the horizontal and vertical arm of BLC in Fig. 13. The design achieved 75% compactness and improved bandwidth at 3.5 GHz. Du and Peng [113] present an ultracompact miniaturized BM based on an electromagnetic MTM transmission line structure. Double spiral line-loop ware used to replace quarter-wavelength TL in BLC design. The network has excellent return loss with an 80.9% BM size reduction compared to the conventional BM. A solid patch BLC and open circuit stub-loaded line on PS was adopted to produce wideband, and the design achieved 16% bandwidth enhancement over 30 GHz frequency of operations.

Fig. 14 shows an ATL incorporated with quasi-lumped elements was used to design a 4 × 4 BM in [114]. The proposed structure was compact with a 79% size reduction at 0.9 GHz frequency. In [115] and [116] a miniaturized 4 × 4 BMs were presented. Compared to the standard design, the size reductions were achieved by replacing conventional TLs with ATL, that resulted in 72.5% and 59.6% miniaturization. A compact 4 × 4 BM was proposed in [117]. ATLs replaced the quarter-wavelength transmission line segment in

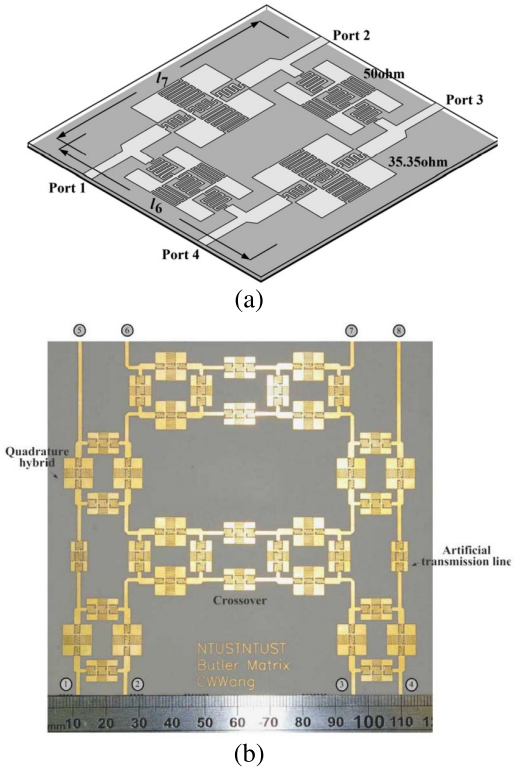

FIGURE 14. Layout diagram of the proposed (a) branch-line coupler and (b) fabricated miniaturized BM [114].

designing BLC. The total area of the proposed matrix is 73.2% less than the traditional design over the 0.9 - 1.1 GHz frequency range. A novel and miniaturized 4 × 4 BM designed with forward wave coupled line coupler and Schiffman PS were proposed in [118]. The structure employs two C-shape and one I-shape defected ground structure (DGS) placed at the ground plane of the couplers and a dumbbell shape DGS at 0dB crossover to enhance the design performance further. The proposed design provides a bandwidth of 120 MHz and occupies an area of 84.74 *mm* × 76.56 *mm* at a 2.4 GHz center frequency.

Table 2 presents the summary of the reported Butler matrices with the reduced number of components. Most of the reviewed articles in this table focused on eliminating crossing and PS to achieve miniaturization and improved bandwidth. However, the essential function of a crossover is to channel the signal from one section to another with high-isolation loss and 0 dB insertion loss. Therefore, the BM without a crossover is expected to provide better performance characteristics in terms of bandwidth improvement, compact size, and phase and amplitude imbalances. Furthermore, avoidance of crossovers will lead to output ports placed at the center of the network; this makes the array element integration difficult and creates chances of interference between the antenna and network surrounding it and affect the element's radiation as demonstrated in [98]. From the analysis of the designed BM without any crossing [98], [99], [100], [101], [102], [103], [104], only article [100] present considerable results with size reduction and slightly improved bandwidth while still maintaining excellent performance characteristics.

Similarly, articles [101], [102], [103], [104] from the table present the design of BM with modified BLC that eliminates phase shifters and crossovers. Most of the techniques demonstrate improved bandwidth and reduce the overall size and complexity of the network. This technique still gravely increases the phase variation and insertion loss as reported by [104]. At the same time the design in [103] shows a deteriorating performance in insertion loss, phase variation, and amplitude imbalance as frequency increases. To conclude, the methods without crossing, without both crossovers, and phase shifters can only be applied in systems operating at a lower frequency, smaller networks, and unsuitable for more extensive BM networks.

Metamaterial structures exhibit unique artificial characteristics not found in nature that are beneficial to microwave devices. Such properties can be utilized extensively to improve microwave devices and circuits' performance characteristics.

Table 3. presents the summary of BM with MTM structure. Based on the analysis, it is understood that most of the articles significantly achieved excellent size reduction and bandwidth improvement. Even though Du and Peng [113] failed to provide information about the system's bandwidth and amplitude imbalance, phase variation is within the required range. From the analysis in table 3, it is evident that increases in the frequency of operation do not have much significant effect on the performance parameters of the network as demonstrated in [109], [110], and [111]. To this end, it was understood and concluded that this technique might be ideal and suitable for both low band mid-band and high band BFN for 5G applications.

Tables 4. Presents a summary of the BM designed using the ATL technique. From the analysis so far, it is understood that ATL-based BM designs demonstrate an excellent size reduction. The method can synthesize microstrip transmission lines by reducing their physical length while maintaining their electrical properties precisely as conventional ones. However, ATL makes the structure design complex and hard to manufacture. It further narrows the operational bandwidth of the system compared to traditional BM as was reported in [114], [115], [116], and [117]. As a result of additional loss due to a large number of discontinuities in the design, thus significantly deteriorating the overall performance. As mentioned earlier in section I, BFN for 5G applications requires wider bandwidth for optimum system performance. This concludes that the ATL-based BM can only provide size miniaturization and not required bandwidth for 5G BF applications.

B. DUAL-BAND BUTLER MATRICES

Characterized by the concurrent service of two or more frequencies in one device, it offers faster speeds and decreases the impact of interference from other devices. With the increasing need for multifrequency, small-sized mobile

TABLE 2. Summarized Butler matrices with decreased number of components.

Ref.	Year	Technique used	Freq. (GHz)	BW (%)	Size reduction (%)	Isolation loss (dB)	Insertion loss (dB)	Phase deviation (°)	Amplitude imbalance (dB)
[98]	2019	BM without CO	35	17.1	-	-17	-	-	-
[99]	2019	4×4 BM without CO	2.44	20.5	-	-15	1	±7	±0.5
‖	‖	8×8 BM without CO	1.9	10.53	-	-15	3	±12	±1.5
[100]	2017	BM without CO	2.5	8	42.68	-20	± 1.5	±3	±1.5
[101]	2019	BM without CO and PS	2	-	79.4	-20	-	±1.74	±0.43
[102]	2019	BM without CO and PS	2	16	68	-32	-	±1	±0.1
[103]	2018	BM without CO and PS	6	37.10	-	-17	-5	±3	±3
[104]	2021	BM without CO and PS	2.56	45.3	80.3	-10	6.8	±7	±1

TABLE 3. Summarized Butler matrices with metamaterial structure.

Ref.	Year	Technique used	Freq. (GHz)	BW (%)	Size reduction (%)	Isolation loss (dB)	Insertion loss (dB)	Phase deviation (°)	Amplitude imbalance (dB)
[105]	2016	4×4 MTM-TL based BM	2.4	8	16.6	-20	-	±4	±2
[106]	2018	4×4 MTM-TL based BM	1.8	-	48	-16	-8.9	-	-
[107]	2018	4×4 MTM-TL based BM	30	30	24	-15	-0.6	±2.5	±0.25
[108]	2019	BM with metasurface layer	28	12.14	-	-25	-3	-	-
[109]	2020	AMC packaged technology	28	7.14	-	-15	-	±10	±5
[111]	2020	4×4 MTM-TL based BM	3.5	15.71	75	-14	-7	±8.7	±2
[112]	2014	4×4 MTM-TL based BM	0.86	-	80.9	-25	-7.6	±4.5	-

terminal devices and multibeam-based stations in 5G mmWave applications, dual-band devices provide broader roaming capabilities. Therefore, several dual-band BM BFN methods are being developed and reported to meet the expectations of these demands.

The first planar dual-band BM was reported in [119]. The proposed design utilizes a dual-band BLC having two parallel coupling lines in which the length of one arm is double the other arm. The phase shifter is made from a TL with meandered curves to provide a proper phase delay, corresponding to the delay of the cascaded crossover and the needed phase shift. Although no effort was made to minimize the size and enhance the bandwidth of the design, the structure demonstrates a good return and isolation losses greater than 20dB operating at 2.4 GHz and 5 GHz frequency bands. In [120], Jizat *et al.* proposed a reduced size dual-band BM using shunt meandered line BLC and PS operating in dual frequency bands of 2.45 GHz and 5.8 GHz. The design provides promising performance with improved bandwidth and covers a total area of 96 $mm \times 125\ mm$ compared to the standard method,

TABLE 4. Summary artificial transmission line-based BM.

Ref.	Year	Technique used	Freq. (GHz)	BW (%)	Size reduction (%)	Isolation loss (dB)	Insertion loss (dB)	Phase deviation (°)	Amplitude imbalance (dB)
[114]	2007	ATL-based BM	0.92	-	79	-32	-8.6	±7.47	-
[115]	2019	ATL-based BM	1	*2.4	72.4	-10	-	±2.5	-
[116]	2019	ATL-based BM	1	*15	59.6	-10	-	±2	-
[117]	2020	ATL-based BM	1	*50	73.15	-10	-	-	9±0

*(*Decreased in operational bandwidth compared to conventional design)*

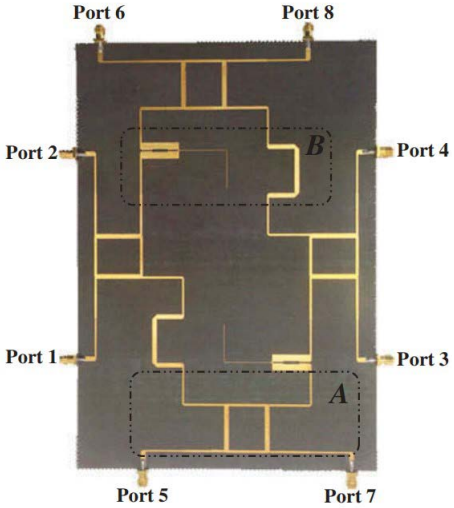

FIGURE 15. Fabricated prototype of 4 × 4 BM [122].

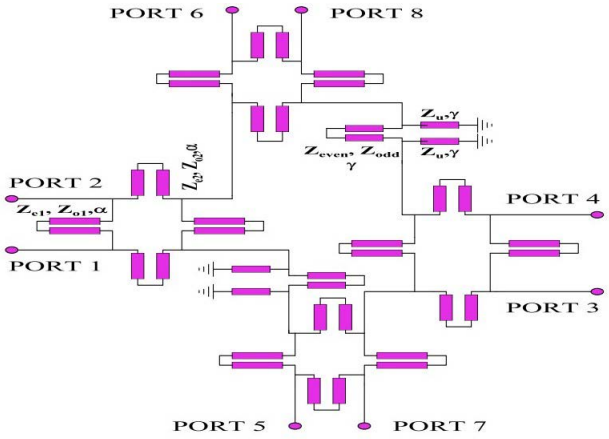

FIGURE 16. Circuit layout of the proposed BM [123].

which is 36% less than the conventional BM. A modified BM with BLCs with different properties in the two frequency bands is proposed as a feeding network in [121]. The structure consists of P radiating elements operating at a higher frequency band and $P/2$ dual-polarized radiating elements operating at a lower frequency band integrated on the same aperture. The proposed structure having $P\times P$ BM at 5.2 GHz and $P/2\times P/2$ BM at 2.4 GHz properly excites the antenna elements. A dual-band BM with the same phase difference for LTE applications is proposed [122]. As shown in Fig. 15, the proposed BM is a 4 × 4 network comprising 3-dB dual-band BLC and 45° broadband PS without CO to operate 1.85 GHz and 2.7 GHz frequency bands. A dual-band 4 × 4 BM that also avoids the use of any crossing is presented in [123]. This design replaced the quarter $\lambda/4$ TL of a single band 3-dB BLC with a dual-band impedance transformer as described in Fig. 16, a short stub was connected at both ends of the coupled line for a dual-band phase shifter design to mitigate band ratio limitations. The structure was compact and achieved 22.3% bandwidth over the 1 GHz and 2.5 GHz frequency bands. Reference [124] proposed a novel branch line coupler equivalent to dual-band ±90° BLC and ±45° phase shifter with 2.3 to 4.4 frequency ratio operations. Its application to develop a dual-band 4 × 4 BM decreases the number of elements and reduces complexity, as shown in Fig. 17.

Table 5. presents the detailed summary of the dual-band BMs. From the analysis in the table, it is understood that dual-band butler matrix for multi-beam systems are designed mainly by converting all primary elements of the single-band BM into their dual-band counterparts; or by creating different radiating elements interleaved together operating at lower and upper-frequency bands. BM can also be developed to operate in a dual-frequency band while producing an excellent performance characteristic. Except for [119] and [122], all other articles in the table demonstrate the compact size and improved bandwidth over 1-6 GHz frequency ranges.

C. SUBSTRATE INTEGRATED WAVEGUIDE (SIW)-BASED BM

K. Wu was the first to propose SIW technology in the early 2000s [125]. SIW presents a class of specific substrate integrated layouts of planar and non-planar systems. It demonstrates that any non-planar system can be incorporated in

TABLE 5. Summary of dualband Butler matrices.

Ref.	Year	Technique used	Freq. (GHz)	BW (%)	Size reduction (%)	Isolation loss (dB)	Insertion loss (dB)	Phase deviation (°)	Amplitude imbalance (dB)
[119]	2005	Dual-band BM	2.4 & 5	-	-	-20	-0.6	±13.5	-
[120]	2013	Dual-band BM	2.45 & 5.8	18.42 & 15.51	36	-24.5 & -14.9	-4 & -3	1 & 2	-
[121]	2016	modified dual-band BM	2.4 & 5.2	2.5 & 3.85	-	-21	-	3	±0.5
[122]	2016	Dual-band BM with same phase difference	1.85 & 2.7	-	-	-15	-	±5.44	±0.72
[123]	2018	Dual-band BM	1 & 2.5	22.3	-	-20	-	±3.14	±0.48
[124]	2020	Dual-band BM using Π-shaped TLs	1 & 2.85	39 & 49	-	-15	-	±3.5	±0.91

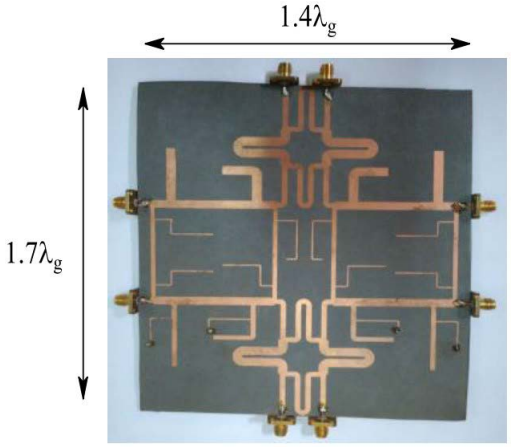

FIGURE 17. Fabricated prototype of 4 × 4 BM [124].

a planar form designed using two equally spaced rows of metallic holes (vias) connecting the bottom and top metallic layers separated by a dielectric substrate. The dispersion and propagation characteristics of SIWs are homogeneous to those of metallic hollow waveguides. Many devices designed for waveguide technology can easily be mimicked using SIWs; this makes them lighter, more straightforward to construct, and less expensive to fabricate than standard hollow waveguides. Nowadays, SIW technology is significantly used to realize BFNs for multi-beam antennas utilizing most of the advantages of hollow waveguides in a planar structure. Recently, T. Paul *et al* proposed a non-planar BM-based BFN for application in the X band frequency range that demonstrated an excellent performance characteristic [126]. However, the structure was bulky and complex to realize, further illustrating the need for a waveguide modeled in planar form.

SIW technology is a good compromise for BM design compared to waveguide or microstrip technologies regarding insertion losses or reduced weight. It suffers the same limitations as rectangular waveguides regarding operational bandwidth. Its valuable bandwidth ranges one-eighth from the cutoff frequency of TE_{10}, which is the fundamental mode, to the cutoff frequency of the second mode TE_{20}; this means the SIW basically operates in a single-mode band [127]. Therefore, the operational bandwidth is narrower than microstrip TL [128]. To improve the SIW bandwidth and reduce the overall size, several SIW structures were reported. In this section, recent developments in SIW-based BM are reported. Size miniaturization, bandwidth enhancement, and different methods to improve performance characteristics are also discussed and presented.

A planar wideband 4 × 4 BM in SIW technology with enhanced power handling on a single layer was proposed in [129]. The structure exhibits a 24% relative bandwidth over the 12.5 GHz frequency, owing to a cruciform SIW quadrature coupler with enhanced bandwidth adopted in the design. SIW based BM was used as a BFN for multi-beam array antennas for 5G mobile devices [130]. In this structure, the overall dimension of the SIW antenna array, including BM, was 72 *mm* × 27.4 *mm* and achieved 4 GHz measured 10 dB bandwidth at 30 GHz frequency with excellent steerable radiation. In SIW BM design, the most convenient approach to build a CO is to have straight delay lines to provide the required phase shift or to cascade two 90° hybrid couplers to make the crossover. However, these approaches increase the circuit size and further complicate the BM design. Another possible technique is to use a curved delay line to provide the desired phase shift as proposed in [131]. As shown in Fig. 18, the designed structure is small with a 74.3 *mm* × 56 *mm* dimension and operates over a 60 GHz frequency band. In [130], a 4 × 4 SIW BM with a modified directional coupler for slot antenna array is proposed for a multi-beam antenna feeder. The modified hybrid coupler was realized using a 90° hybrid coupler followed by a −45° phase shifter that outputs 45° /135° output phase difference. The design exhibits miniaturization of the overall structure with

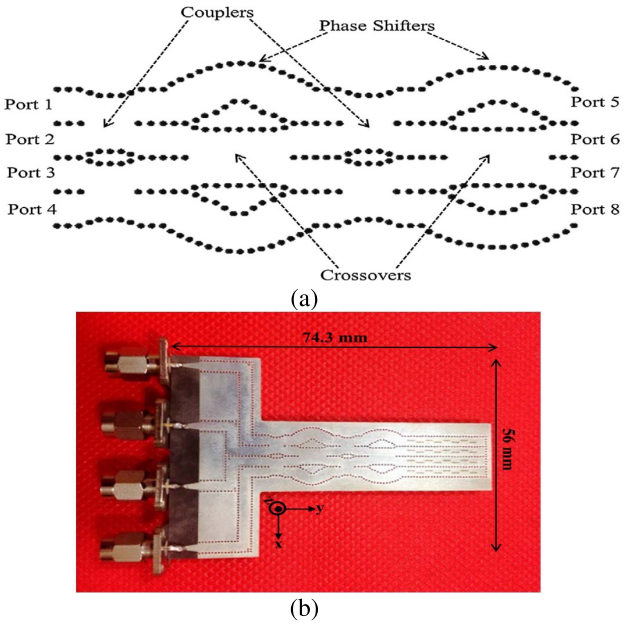

FIGURE 18. Layout of (a) SIW BM structure (b) fabricated multibeam antenna [131].

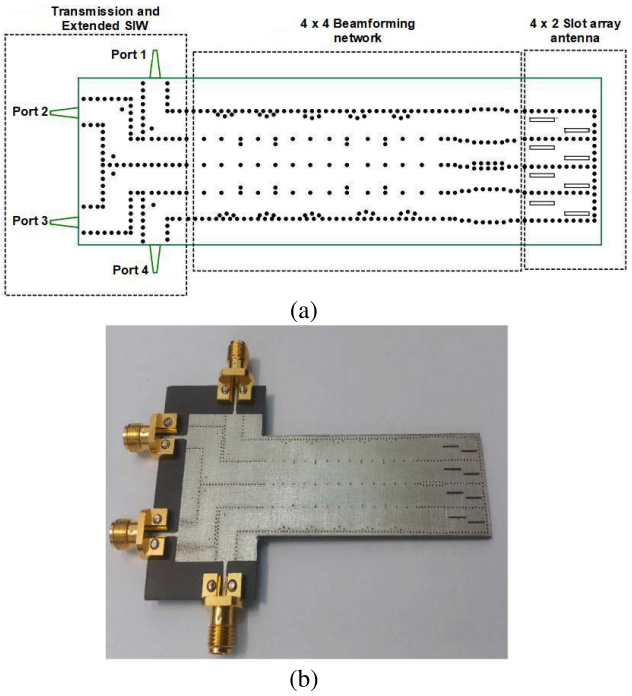

FIGURE 19. (a) Circuit layout of the proposed design. (b) Fabricated prototype of the structure [133].

110 *mm* × 42 *mm* dimensions over the 28-32 GHz frequency range. Article [132] presents SIW based BM to operate within the 27.75 - 28.25 GHz frequency range. The 4 × 4 BM structure consists of four 90° couplers, two crossovers, and two 135° phase shifters made by cascading two hybrid couplers. The lateral size of the BM structure is 100.59 *mm* × 50.75 *mm* at 28 GHz center frequency. In their effort to reduce the structure size, Pezhman [133] proposed a novel compact 4 × 4 SIW based BM using a single layer approach. The novelty of the design was eliminating the CO sections and developing a BM on fewer components based on a 4 × 4 multiple-aperture coupler (MAC) in cascade with a 4 × 4 PS. The proposed structure shown in Fig. 19 demonstrates a significant size reduction with a total area of 56.5 *mm* × 21 *mm*, including the antenna, which is a 33% reduction in size compared to similar designs. The work in [134] proposed a compact and broadband 4 × 4 substrate integrated waveguide Butler matrix with phase and magnitude error reductions. The method uses a dual-layer approach to achieve compactness covering a 55 *mm* × 34 *mm* total area with a 22% bandwidth improvement. It avoided using a length-line for size reduction, which increases the output phase error. In [135], the design achieved miniaturization by eliminating the CO and using a dual-layer approach in designing an 8 × 8 SIW based BM that resulted in 50% size reduction and 10% useful bandwidth at the 30 GHz frequency band. To decrease the longitudinal length, the design proposed in [136] introduced an interdigital slot (IDS) in the SIW transmission line. It produced a TE_{10}/TE_{20} dual-mode that can be controlled by optimizing the size of the slots and varying the difference between the phase constant of the two modes. As a result, the coupling region was shortened, and

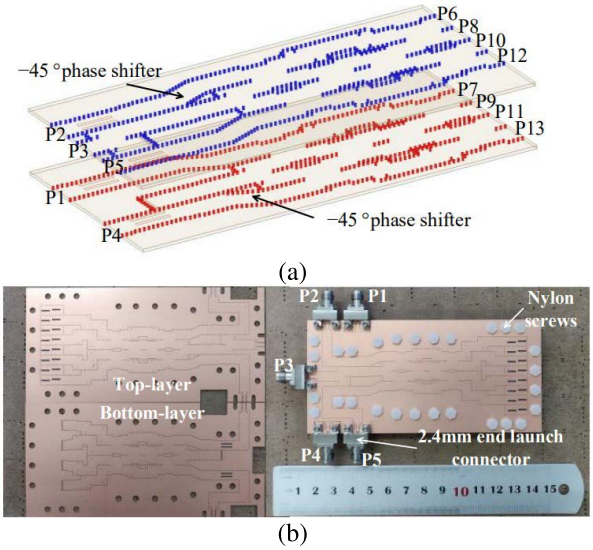

FIGURE 20. (a) Layout diagram of the proposed BM. (b) Fabricated prototype [137].

miniaturization was obtained. The overall structure size is reduced by 29% and operates over a 30 GHz frequency band.

A 5 × 8 BM based on SIW technology was proposed in [137]. In this design, the BM was constructed directly by combining two 3 × 4 BMs, a power divider, and two 3 dB couplers with the top layer (in blue) and bottom layer (in red), as illustrated in Fig. 20. The proposed design was compact with a 27.46 *mm* × 63.69 *mm* structure size at 26 GHz center frequency. By adopting the dual-layer approach, the size and

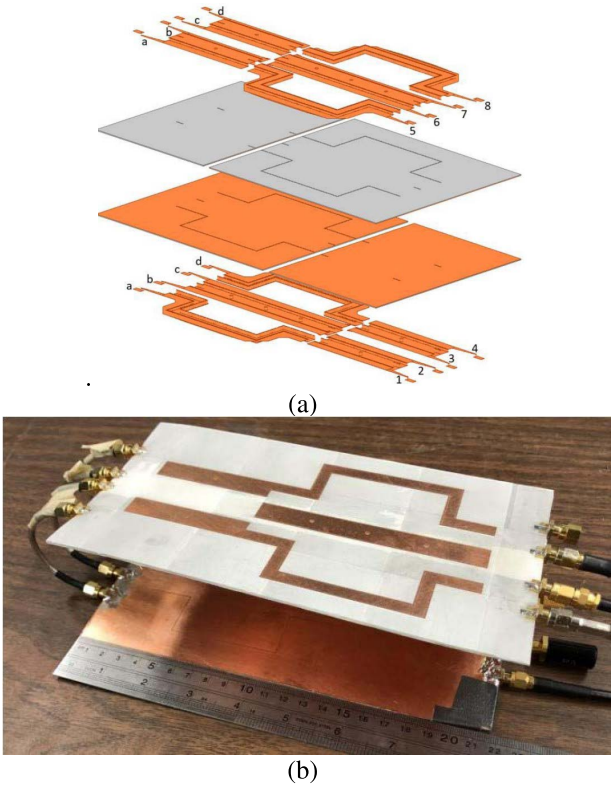

FIGURE 21. Layout diagram of the proposed (a) branch-line coupler and (b) fabricated miniaturized BM [138].

complexity of the BM were effectively reduced, and about 10.2% bandwidth was also reported over the 27.8 – 30.8 GHz frequency range. In [139], a compact mmWave endfire array antenna with dual-polarization for multibeam applications is proposed. A dualmode SIW segment with dual-mode excitation is obtained by inserting a metal layer in the middle of the conventional SIW; this can be considered as two stacked SIWs. The structure was used as a feeder to endfire array and achieved the 11.3% bandwidth improvement with 27.4 *mm* × 69.63 *mm* overall dimensions.

Another means to minimize the size of SIW is to fold the SIW structure around metal support, forming C-shaped; thus, referred to as substrate integrated folded waveguide (SIFW) as proposed in [140]. This method led to the 40% reduction in size and required a multilayer approach that demonstrated an excellent performance. To further miniaturize and enhance the bandwidth performance of classical SIW technology, the substrate integrated ridge waveguide (SIRW) was proposed in [141], [142], and [138]. This structure is a dual-layer topology that uses fragmented in-length metal vias forming ridge in the wall of the SIW. The design in [141] exhibits a 20% bandwidth over the 30 GHz frequency band, and the overall BM size was reported to be 5.6 $\lambda \times 7.1\ \lambda$. In [138], a miniaturized 4 × 4 BM using ridged half-mode SIW was proposed. As shown in Fig. 21, the design topology achieved miniaturization through the transverse resonance technique and the capacitive ridge introduction that resulted in a 5% bandwidth and 70% size reduction compared to the full-mode SIW.

Table 6 gives a detailed summary of some of the SIW Butler matrices. Different innovative techniques from previous works of literature to improve compactness, wideband, and other critical performance parameters were presented. It is evident that SIW BM technology demonstrates excellent performance in terms of size reduction and insertion loss. However, even though most articles are designed at a high-frequency, greater than 25 GHz, the realized bandwidth is relatively narrow. Multilayer structure demonstrates a greater level of compactness and shows improved bandwidth as in [140]. Finally, articles [138], [141], [142] presents an encouraging solution for implementing better bandwidth and miniaturization beam steering devices for 5G applications.

D. GAP WAVEGUIDE (GWG)-BASED BUTLER MATRICES

The beam scanning potential of multibeam antennas can be realized using RF-BFNs and enhance the utilization of spectrum resources. However, when working at higher frequencies in mmWave bands, the dielectric loss and radiation loss increases significantly when the BFNs are based on the traditional microstrip line technique. SIW technology has been used to obtain lower transmission loss at the mmWave band, yet suffers from the dielectric loss due to the substrate material.

The GWG is an emerging technology proposed by *Per-Simon Kildal* in 2009 [143]. It is relatively a waveguide structure consisting of two semi-enclosed contactless surfaces. The metallic plate at the bottom is replaced by a high impedance perfect magnetic conductor (PMC) structure with a textured of square metallic nails. At the top of the structure, a metallic plate acting as a perfect electric conductor (PEC) is placed such that at a distance less than $\lambda/4$ no propagation of electromagnetic waves between the two surfaces. The propagation characteristics of GWG below and above cutoff were investigated [144], and the typical structural diagrams are shown in Fig. 22. The GWG technology, which includes ridge gap waveguide (RGW) and groove gap waveguide (GGW) technologies, has tremendous advantages of low loss, low fabrication difficulty, and easy assembly than the SIW technology as frequencies increases [145]. It has broad imminent applications in the designs of both active, passive devices, and complex networks at mmWave and sub-mmWave frequencies. The GWG structure can be designed simply by adequately positioning the nails that define the groove, and the signal mostly travels in the air without leakage losses.

An initial work that employed the GWG technique in BM design using inverted microstrip on a ridge was reported in [146]. The structure presents the easy translation of typical microstrip devices and circuits with enhanced performance. As mentioned earlier, using the classical groove version provides several advantages concerning losses as the frequency increases. Therefore, the design of 4 × 4 BM's components in GWG technology was proposed in [147]. All the components are wideband and demonstrate good performance over

TABLE 6. Summary of substrate integrated waveguide (SIW) Butler matrices.

Ref.	Year	Technique used	Freq. (GHz)	BW (%)	Dimensions (mm^2)	Isolation loss (dB)	Insertion loss (dB)	Phase deviation (°)
[129]	2011	SIW technology	12.5	24	144 × 145	20	-	15
[130]	2016	SIW technology	30	13.33	72 × 27.4	-	-	20
[131]	2016	SIW technology	60	11.67	74.3 × 56	10	-	-
[132]	2020	SIW technology	28	1.6	9.39 λ × 4.74 λ	23	-	11.1
[133]	2021	SIW & MAC	30	13.3	56.5 × 21	13	-	-
[134]	2015	Two layer SIW technology	9	22	55 × 34	15	-	5
[135]	2017	Dual layer 8 × 8 SIW technology	30	10	10 λ × 4 λ	10	-	-
[136]	2021	CRLH-TL SIW technology	30	-	0.76 λ × 2.96 λ	12	-	11
[137]	2020	Multilayer SIW technology	26	11.3	27.46 × 63.69	10	-	-
[138]	2020	Ridge half-mode SIW	3.5	5	11.4 λ × 11.4 λ	26.5	2.2	22
[139]	2021	5 × 8 multilayer SIW technology	29	10.2	27.4 × 63.5	15	9	9.8
[140]	2020	multilayer folded C-type SIW	30	-	1.24 λ × 5.54 λ	18	-0.16	2
[141]	2020	Printed ridge waveguide	30	20	5.6 λ × 7.1 λ	15	-	5

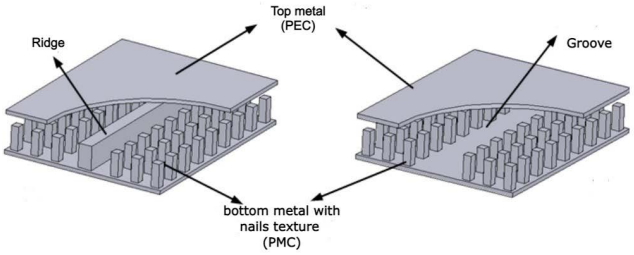

FIGURE 22. Groove gap and ridge gap waveguide structures [145].

the 26 GHz frequency band. A wideband 4 × 4 BM in the printed (RGW) was reported in [142]. As shown in Fig. 23, the structure is compact and achieved 21.25% bandwidth centered at a 30 GHz frequency band.

Another full metallic RGW 4 × 4 BM was presented in [148]. The simulated results from the design demonstrated an excellent performance over the 24 GHz to 28 GHz frequency range. Zarifi *et al.* [149] proposed a 4 × 4 BM based on RGW for applications in the 60 GHz frequency range. The structure shown in Fig. 24 is made from four 3-dB couplers, four PSs, and two COs. The two additional PS inserted before the output ports 5 and 8 provide appropriate progressive phases at the output.

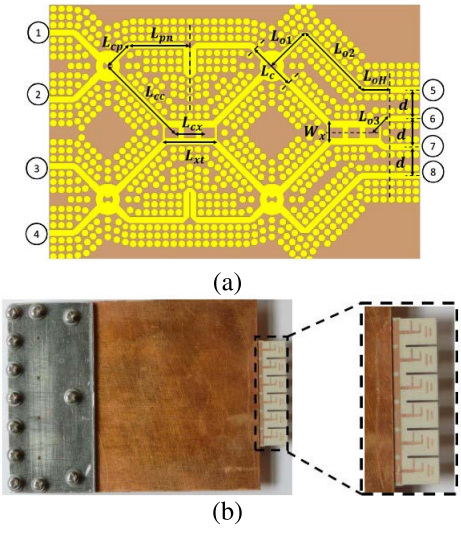

FIGURE 23. Layout diagram of the proposed (a) BM and (b) fabricated BM [142].

In [150], a GGW-based cross-polarization array antenna is fed with GGW BM to develop a wideband multibeam antenna at the 83 GHz frequency band. A multi-layer GGW-based BM is employed as a feeding network for leaky-wave

TABLE 7. Summary of gap waveguide (GWG) Butler matrices.

Ref.	Year	Technique used	Freq. (GHz)	BW (%)	Dimensions (mm)	Isolation loss (dB)	Phase deviation ($^\circ$)	Amplitude imbalance (dB)
[146]	2015	Inverted microtrip in RGW	60	-	-	-	-	-
[147]	2017	RGW technology	26	-	-	-	-	-
[142]	2020	GGW technology	30	21.25	90×54	< -10	$\pm 10^\circ$	± 1.6
[148]	2022	RGW technology	26	15.40	-	-15	$\pm 6^\circ$	± 1
[149]	2021	RGW technology	60	3.33	-	-15	$\pm 7^\circ$	± 1
[150]	2021	GGW technology	85	17.6	-	< -15	$\pm 17^\circ$	± 1.5
[151]	2021	Multi-layer GGW technology	30	30	-	< -10	-	-
[152]	2020	Asymmetric BM in GGW technology	94	0.7	160×100	-23	$\pm 20^\circ$	± 0.8

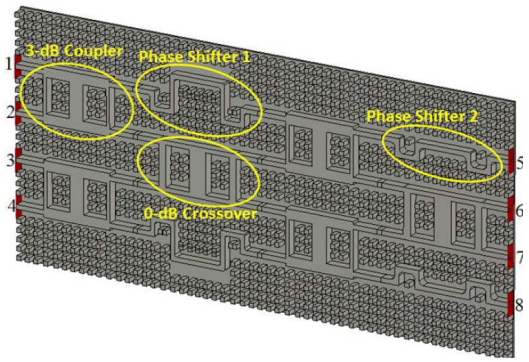

FIGURE 24. Proposed BM structure [149].

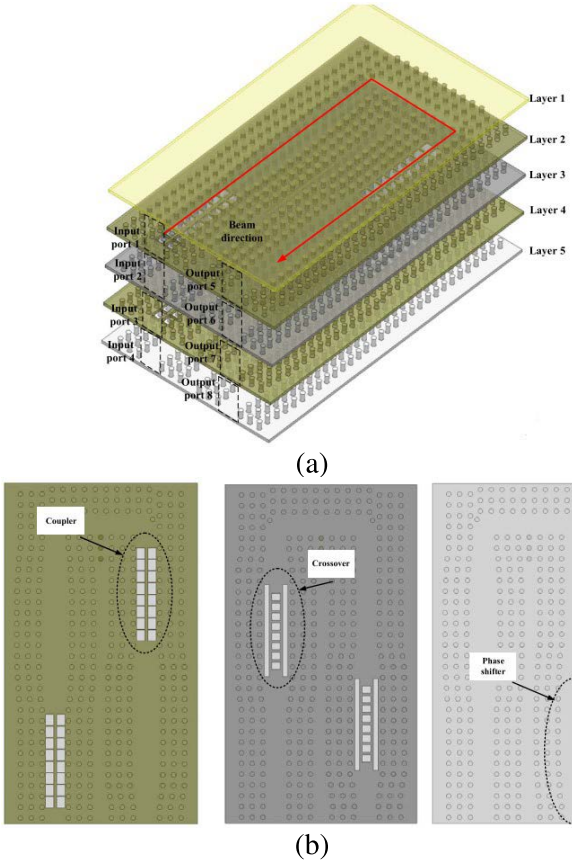

FIGURE 25. Layout diagram of the proposed (a) overall multi-layer BM and (b) different layers of the design [151].

array antenna in [151]. Each component of BM is on a different layer, and the BM is designed using a 3-D design fabrication technique, as shown in Fig. 25. The article in [152] presents a modified BM in 3-D GGW technology as shown in Fig. 26 the BM structure is asymmetric and designed to operate at 94 GHz for radar applications.

Therefore, one can observe the progressive development of BM based on GWG technology. A detailed summary of some of the BMs designed based on GGW is presented in Table 7. Algaba-Brazalez and Rajo-Iglesias [146] and Bernal and Rajo-Iglesias [147] show the early stage of BM design in GWG technology, where BM components such as couplers, phase shifters, and crossovers are developed at high frequencies without complete BM integration. All the remaining articles from the table present the fully integrated BM using GWG technology. From the table, it was deduced that amplitude imbalance is below 2 dB; this indicates the low loss nature of the technique as we go further up in the frequency range. Similarly, excellent operational bandwidth was achieved using this technique, especially the multi-layer approach reported in [151]. Except in the article [152],where the narrow bandwidth and high phase error were due to the design's asymmetry between the input and output ports. Therefore, it can be concluded that the GGW technique is a

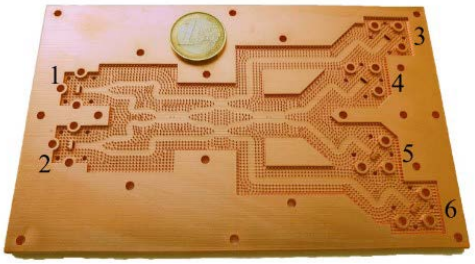

FIGURE 26. Proposed 3-D BM structure [152].

good candidate for BM design in mmWave and sub-mmWave frequency bands.

V. CONCLUSION AND FUTURE WORK

This paper reviews recent progress in RF-BFNs, focusing on beamforming network developed from the Butler matrices. Components that include BLCs, phase shifters, and crossovers for BM implementation were relatively discussed. Microwave devices built from microstrip transmission lines usually occupy large circuit areas, exhibits narrow bandwidth, and high transmission losses especially at high frequency ranges. Since then, many researchers have developed distinctive and innovative design methods to mitigate the challenges and improve the network performance. From the literature, it was found that MTM-based structure provides better performance in terms of insertion loss, phase deviation, and fabrication cost with an additional degree of freedom in miniaturization. Furthermore, MTM themselves are classified into resonant and nonresonant types structures. The resonant types such as SRRs and CSRRs generally exhibit narrow bandwidth and high loss. The quality factor associated with the resonator, which is related to transmission, has an unavoidable trade-off between transmission level and the operational bandwidth [153]. The loaded quality factor (total transmission loss) in a resonator is equal to the summation of the losses due to external circuits (source/load) coupling and the ohmic/dielectric losses.

Similarly, the loaded quality factor, which is actually a figure of merit in terms of transmission is inversely proportional to the operational bandwidth, and is also derived from the magnitude of S_{21}. The maximum quality factor is achieved by decreasing the bandwidth at the resonance frequency. Therefore, resonant structures do not represent a good propagating medium for modulated signal. Consequently, nonresonant type MTM TL structures such as CRLH TL provides planar configurations with simultaneous wide bandwidth and low loss suitable for modern microwave applications.

Each of these elements contributes to overall BM circuit performance. The analysis also found that BM can be made to operate at two different frequency bands. Simply by converting each single-band component to its dual-band counterpart. However, it is understood that most of the techniques are performed with small frequency ratios (<3). In practical applications, enlarging the frequency ratio and maintaining a compact structure without deteriorating performance is paramount. Furthermore, most reported works in the literature were conducted below sub-6 GHz 5G, above which the system will be virtually impractical to implement due to fabrication tolerances. Another promising research direction for BM design in the upper 5G frequency range bands is to employ SIW technology. SIW BM has better insertion loss, low implementation cost, and high-power capacity. Yet, most designs operate at a higher frequency and suffer from bandwidth limitations due to similarities with the rectangular waveguides. Therefore, innovative methods for bandwidth enhancement and dual-band enabling of SIW BM is great future direction. Recently, the groove gap waveguide technology proved to be feasible solution in terms of losses and low manufacturing cost regardless of the design frequencies. This is due to the fact that GGW has no substrate and waves mainly propagate through air. Therefore, each reported technique from the analysis has advantages and disadvantages regarding deployment into the desired frequency spectrum.

REFERENCES

[1] J. Zhao, S. Ni, L. Yang, Z. Zhang, Y. Gong, and X. Yu, "Multiband cooperation for 5G HetNets: A promising network paradigm," *IEEE Veh. Technol. Mag.*, vol. 14, no. 4, pp. 85–93, Dec. 2019.

[2] S. Mattisson, "Overview of 5G requirements and future wireless networks," in *Proc. 43rd IEEE Eur. Solid State Circuits Conf. (ESSCIRC)*, Sep. 2017, pp. 1–6.

[3] Y. Li, C.-Y.-D. Sim, Y. Luo, and G. Yang, "12-port 5G massive MIMO antenna array in sub-6 GHz mobile handset for LTE bands 42/43/46 applications," *IEEE Access*, vol. 6, pp. 344–354, 2017.

[4] Z. Ren, S. Wu, and A. Zhao, "Coexist design of sub-6 GHz and millimeter-wave antennas for 5G mobile terminals," in *Proc. Int. Symp. Antennas Propag. (ISAP)*. 2018, pp. 1–2.

[5] R. J. Mailloux, *Phased Array Antenna Handbook*. Norwood, MA, USA: Artech House, 2017.

[6] A. Bhattacharyya, *Phased Array Antennas: Floquet Analysis, Synthesis, BFNs and Active Array Systems*. Hoboken, NJ, USA: Wiley, 2006, pp. 53–56.

[7] M. N. Hamdy, "Beamformers explained," Commscope, Hickory, NC, USA, White Paper 114491-EN,(06/00), 2020.

[8] S. Sun and T. S. Rappaport, "Multi-beam antenna combining for 28 GHz cellular link improvement in urban environments," in *Proc. IEEE Global Commun. Conf. (GLOBECOM)*, Dec. 2013, pp. 3754–3759.

[9] G. Babur, G. O. Manokhin, A. A. Geltser, and A. A. Shibelgut, "Low-cost digital beamforming on receive in phased array radar," *IEEE Trans. Aerosp. Electron. Syst.*, vol. 53, no. 3, pp. 1355–1364, Jun. 2017.

[10] V. Venkateswaran and A.-J. Van Der Veen, "Analog beamforming in MIMO communications with phase shift networks and online channel estimation," *IEEE Trans. Signal Process.*, vol. 58, no. 8, pp. 4131–4143, Aug. 2010.

[11] I. Ahmed, H. Khammari, A. Shahid, A. Musa, K. S. Kim, E. De Poorter, and I. Moerman, "A survey on hybrid beamforming techniques in 5G: Architecture and system model perspectives," *IEEE Commun. Surveys Tuts.*, vol. 20, no. 4, pp. 3060–3097, 4th Quart., 2018.

[12] K. Zarb-Adami, A. Faulkner, J. G. Bij De Vaate, G. W. Kant, and P. Picard, "Beamforming techniques for large-N aperture arrays," in *Proc. IEEE Int. Symp. Phased Array Syst. Technol.*, Oct. 2010, pp. 883–890.

[13] L. Kuai, J. Chen, Z. H. Jiang, C. Yu, C. Guo, Y. Yu, H.-X. Zhou, and W. Hong, "A N260 band 64 channel millimeter wave full-digital multi-beam array for 5G massive MIMO applications," *IEEE Access*, vol. 8, pp. 47640–47653, 2020.

[14] R. Zhang, J. Zhou, J. Lan, B. Yang, and Z. Yu, "A high-precision hybrid analog and digital beamforming transceiver system for 5G millimeter-wave communication," *IEEE Access*, vol. 7, pp. 83012–83023, 2019.

[15] E. H. Mujammami, I. Afifi, and A. B. Sebak, "Optimum wideband high gain analog beamforming network for 5G applications," *IEEE Access*, vol. 7, pp. 52226–52237, 2019.

[16] W. T. Sethi, A. B. Ibrahim, K. Issa, and S. A. Alshebeili, "MmW Rotman lens-based sensing: An investigation study," *Sensors*, vol. 21, no. 4, p. 1163, Feb. 2021.

[17] C. Tsokos, E. Mylonas, P. Groumas, V. Katopodis, L. Gounaridis, R. B. Timens, R. M. Oldenbeuving, C. G. Roeloffzen, H. Avramopoulos, and C. Kouloumentas, "Analysis of a multibeam optical beamforming network based on Blass matrix architecture," *J. Lightw. Technol.*, vol. 36, no. 16, pp. 3354–3372, Aug. 15, 2018.

[18] H. Ren, H. Zhang, and B. Arigong, "Ultra-compact 3 × 3 Nolen matrix beamforming network," *IET Microw., Antennas Propag.*, vol. 14, no. 3, pp. 143–148, Feb. 2020.

[19] V. M. Jayakrishnan and S. K. Menon, "Realization of Butler matrix for beamforming in phased array system," *Proc. Comput. Sci.*, vol. 93, pp. 223–229, 2016.

[20] N. J. G. Fonseca, "Discussion on reciprocity, unitary matrix, and lossless multiple beam forming networks," *Int. J. Antennas Propag.*, vol. 2015, pp. 1–9, Apr. 2015.

[21] J. Blass, "Multidirectional antenna-a new approach to stacked beams," in *Proc. IRE Int. Conv. Rec.*, vol. 8, Mar. 1966, pp. 48–50.

[22] N. J. G. Fonseca, A. Ali, and H. Aubert, "Cancellation of beam squint with frequency in serial beamforming network-fed linear array antennas," *IEEE Antennas Propag. Mag.*, vol. 54, no. 1, pp. 32–39, Feb. 2012.

[23] F. Casini, R. V. Gatti, L. Marcaccioli, and R. Sorrentino, "A novel design method for Blass matrix beam-forming networks," in *Proc. Eur. Microw. Conf.*, 2007, pp. 1511–1514.

[24] D. Lialios, C. L. Zekios, S. V. Georgakopoulos, C. I. Kolitsidas, K. D. Paschaloudis, A. G. Koutinos, and G. A. Kyriacou, "A mm-wave true-time-delay beamformer architecture based on a Blass matrix topology," in *Proc. IEEE Int. Symp. Antennas Propag. North Amer. Radio Sci. Meeting*, Jul. 2020, pp. 1609–1610.

[25] D. I. Lialios, N. Ntetsikas, K. D. Paschaloudis, C. L. Zekios, S. V. Georgakopoulos, and G. A. Kyriacou, "Design of true time delay millimeter wave beamformers for 5G multibeam phased arrays," *Electronics*, vol. 9, no. 8, p. 1331, Aug. 2020.

[26] N. J. Fonseca, "Printed S-band 4 × 4 Nolen matrix for multiple beam antenna applications," *IEEE Trans. Antennas Propag.*, vol. 57, no. 6, pp. 1673–1678, Jun. 2009.

[27] J. Nolen, *Synthesis of Multiple Beam Networks For Arbitrary Illuminations*. Avon, Ohio: Bendix, 1965.

[28] F. E. Fakoukakis and G. A. Kyriacou, "Novel Nolen matrix based beamforming networks for series-fed low SLL multibeam antennas," *Prog. Electromagn. Res. B*, vol. 51, pp. 33–64, Apr. 2013.

[29] A. Ali, N. Fonseca, F. Coccetti, and H. Aubert, "Novel two-layer 4 × 4 SIW Nolen matrix for multi-beam antenna application in Ku band," in *Proc. 3rd Eur. Conf. Antennas Propag.*, 2009, pp. 241–243.

[30] H. Ren, H. Zhang, Y. Jin, Y. Gu, and B. Arigong, "A novel 2-D 3 × 3 Nolen matrix for 2-D beamforming applications," *IEEE Trans. Microw. Theory Techn.*, vol. 67, no. 11, pp. 4622–4631, Nov. 2019.

[31] W. C. Cummings, "Multiple beam forming networks," Massachusetts Inst. Tech. Lexington Lincoln Lab, Lexington, MA, USA, Tech. Rep., 1978.

[32] Y. J. Guo, M. Ansari, and N. J. G. Fonseca, "Circuit type multiple beamforming networks for antenna arrays in 5G and 6G terrestrial and non-terrestrial networks," *IEEE J. Microw.*, vol. 1, no. 3, pp. 704–722, Jul. 2021.

[33] J. Butler, "Beam-forming matrix simplifies design of electronically scanned antenna," *Electron Des.*, vol. 9, no. 7, pp. 170–173, 1961.

[34] A. K. Vallappil, M. K. A. Rahim, B. A. Khawaja, N. A. Murad, and M. G. Mustapha, "Butler matrix based beamforming networks for phased array antenna systems: A comprehensive review and future directions for 5G applications," *IEEE Access*, vol. 9, pp. 3970–3987, 2020.

[35] G. Adamidis and I. Vardiambasis, "Design and implementation of a 4 × 4 Butler-matrix switched-beam antenna array at the microwave communications and electromagnetic applications lab of the technological educational institute of Crete," Tech. Educ. Inst., Chania, Greece, Tech. Rep., 2005.

[36] T.-G. Ma, C.-W. Wang, C.-H. Lai, and Y.-C. Tseng, "Periodic synthesized transmission lines with two-dimensional routing," in *Synthesized Transmission Lines: Design, Circuit Implementation, and Phased Array Applications*. Singapore: Wiley, 2019, p. 168.

[37] J. Lim, J. Lee, Y. Jeon, K. Kwon, S.-M. Han, D. Ahn, and Y. Jeong, "Design of a miniaturized branch line coupler using common defected ground structure," in *Proc. IEEE Int. Symp. Antennas Propag.*, Jul. 2012, pp. 1–2.

[38] A. C. Das, L. Murmu, and S. Dwari, "A compact branch-line coupler using folded microstrip lines," in *Proc. Int. Conf. Microw. Photon. (ICMAP)*, Dec. 2013, pp. 1–3.

[39] M. Moubadir, H. Aziz, N. A. Touhami, and A. Mohamed, "A miniaturized branch-line hybrid coupler microstrip for long term evolution applications," *Proc. Manuf.*, vol. 22, pp. 491–497, 2018.

[40] A. Sardi, J. Zbitou, A. Errkik, and M. Latrach, "Design and fabrication of the novel miniaturized microstrip coupler 3dB using stepped impedance resonators for the ISM applications," *TELKOMNIKA Telecommun. Comput. Electron. Control*, vol. 16, no. 4, p. 1560, Aug. 2018.

[41] H. A. Mohamed and A. S. Mohra, "Compact cascaded branch line coupler using T-sections conversion," in *Proc. 34th Nat. Radio Sci. Conf. (NRSC)*, Mar. 2017, pp. 64–70.

[42] D. Letavin, "Miniature microstrip branch line coupler with folded artificial transmission lines," *AEU Int. J. Electron. Commun.*, vol. 99, pp. 8–13, Feb. 2019.

[43] K. V. P. Kumar and S. S. Karthikeyan, "Wideband three section branch line coupler using triple open complementary split ring resonator and open stubs," *Int. J. Electron. Commun.*, vol. 69, no. 10, pp. 1412–1416, 2015.

[44] L. Geng, G.-M. Wang, P. Peng, and Y.-W. Wang, "Design of miniaturized branch-line coupler based on novel composite right/left-handed transmission line structure," in *Proc. IEEE Int. Conf. Comput. Electromagn. (ICCEM)*, Mar. 2019, pp. 1–3.

[45] A. K. Vallappil, M. K. A. Rahim, B. A. Khawaja, and M. Aminu-Baba, "Metamaterial based compact branch-line coupler with enhanced bandwidth for use in 5G applications," *Appl. Comput. Electromagn. Soc. J.*, vol. 35, pp. 700–708, Jun. 2020.

[46] K.-K. Cheng and F.-L. Wong, "A novel approach to the design and implementation of dual-band compact planar 90° branch-line coupler," *IEEE Trans. Microw. theory Techn.*, vol. 52, no. 11, pp. 2458–2463, Nov. 2004.

[47] N. Zheng, L. Zhou, and W.-Y. Yin, "A novel dual-band Π-shaped branch-line coupler with stepped-impedance stubs," *Prog. Electromagn. Res. Lett.*, vol. 25, pp. 11–20, Jun. 2011.

[48] C.-H. Yu and Y.-H. Pang, "Dual-band unequal-power quadrature branch-line coupler with coupled lines," *IEEE Microw. Wireless Compon. Lett.*, vol. 23, no. 1, pp. 10–12, Jan. 2012.

[49] H. Zhang, W. Kang, and W. Wu, "A novel compact dual-band branch-line coupler with cross-shaped stubs," in *Proc. IEEE Int. Conf. Ubiquitous Wireless Broadband (ICUWB)*, Oct. 2016, pp. 1–4.

[50] A. M. Zaidi, M. T. Beg, B. K. Kanaujia, K. Srivastava, and K. Rambabu, "A dual band branch line coupler with wide frequency ratio," *IEEE Access*, vol. 7, pp. 25046–25052, 2019.

[51] L. Xia, J.-L. Li, B. A. Twumasi, P. Liu, and S.-S. Gao, "Planar dual-band branch-line coupler with large frequency ratio," *IEEE Access*, vol. 8, pp. 33188–33195, 2020.

[52] S. Amiri, M. Kamyab-Hesari, and M. Dousti, "A novel highly compact dual-band branch-line coupler utilizing left and right-handed technique," in *Proc. Annu. IEEE India Conf.*, Dec. 2011, pp. 1–4.

[53] M. S. Ghaffarian, G. Moradi, S. Khajehpour, M. M. Honari, and R. Mirzavand, "Dual-band/dual-mode rat-race/branch-line coupler using split ring resonators," *Electronics*, vol. 10, no. 15, p. 1812, Jul. 2021.

[54] Y. K. Jung and B. Lee, "Dual-band circularly polarized microstrip RFID reader antenna using metamaterial branch-line coupler," *IEEE Trans. Antennas Propag.*, vol. 60, no. 2, pp. 786–791, Feb. 2011.

[55] A. Koelpin, B. Pape, and R. Weigel, "Introducing new design guidelines for dualband CRLH structures formed by transmission lines and lumped components," in *IEEE MTT-S Int. Microw. Symp. Dig.*, Sep. 2009, pp. 1–4.

[56] S. Barth and A. K. Iyer, "A dual-band quadrature hybrid coupler using embedded MTM-EBGs," in *Proc. IEEE Int. Symp. Antennas Propag. USNC/URSI Nat. Radio Sci. Meeting*, Jul. 2018, pp. 199–200.

[57] M. K. Khattak, C. Lee, H. Park, and S. Kahng, "A fully-printed CRLH dual-band dipole antenna fed by a compact CRLH dual-band balun," *Sensors*, vol. 20, no. 17, p. 4991, Sep. 2020.

[58] F. Akbar and A. Mortazawi, "A frequency tunable 360° analog CMOS phase shifter with an adjustable amplitude," *IEEE Trans. Circuits Syst., II, Exp. Briefs*, vol. 64, no. 12, pp. 1427–1431, Dec. 2017.

[59] Y. Jiang, X. Q. Lin, B. Wang, and C. Tang, "Theoretical analysis and design of a compact analogue phase shifter with constant low insertion loss," *Electron. Lett.*, vol. 54, no. 8, pp. 517–519, Apr. 2018.

[60] J. Zhou, H. J. Qian, and X. Luo, "High-resolution wideband vector-sum digital phase shifter with on-chip phase linearity enhancement technology," *IEEE Trans. Circuits Syst. I, Reg. Papers*, vol. 68, no. 6, pp. 2457–2469, Jun. 2021.

[61] B. M. Schiffman, "A new class of broad-band microwave 90-degree phase shifters," *IRE Trans. Microw. Theory Techn.*, vol. 6, no. 2, pp. 232–237, Apr. 1958.
[62] D. M. Pozar, "Electromagnetic theory," in *Microwave Engineering*, vol. 4, 2nd ed. 1998, pp. 1–42.
[63] Y.-X. Guo, Z.-Y. Zhang, and L. Ong, "Improved wide-band Schiffman phase shifter," *IEEE Trans. Microw. Theory Techn.*, vol. 54, no. 3, pp. 1196–1200, Mar. 2006.
[64] Z. Zhang, Y.-C. Jiao, S.-F. Cao, X.-M. Wang, and F.-S. Zhang, "Modified broadband Schiffman phase shifter using dentate microstrip and patterned ground plane," *Prog. Electromagn. Res. Lett.*, vol. 24, pp. 9–16, May 2011.
[65] Y.-P. Lyu, L. Zhu, and C.-H. Cheng, "Design and analysis of Schiffman phase shifter under operation of its second phase period," *IEEE Trans. Microw. Theory Techn.*, vol. 66, no. 7, pp. 3263–3269, Jul. 2018.
[66] L.-L. Qiu, L. Zhu, and Y.-P. Lyu, "Schiffman phase shifters with wide phase shift range under operation of first and second phase periods in a coupled line," *IEEE Trans. Microw. Theory Techn.*, vol. 68, no. 4, pp. 1423–1430, Apr. 2019.
[67] P. K. Deb, T. Moyra, and B. K. Bhattacharyya, "Design of compact wide-band 90° Schiffman phase shifter incorporating CSRR," *Electromagnetics*, vol. 40, no. 3, pp. 207–216, Apr. 2020.
[68] X. Tang and K. Mouthaan, "Dual-band class III loaded-line phase shifters," in *Proc. Asia–Pacific Microw. Conf.*, 2010, pp. 1731–1734.
[69] K. Rawat and F. M. Ghannouchi, "Design methodology for dual-band Doherty power amplifier with performance enhancement using dual-band offset lines," *IEEE Trans. Ind. Electron.*, vol. 59, no. 12, pp. 4831–4842, Dec. 2011.
[70] H. Ren, J. Shao, M. Zhou, B. Arigong, J. Ding, and H. Zhang, "Design of dual-band transmission line with flexible phase shifts and its applications," *IET Electron. Lett.*, vol. 51, no. 3, pp. 261–262, Feb. 2015.
[71] Y.-P. Lyu, L. Zhu, and C.-H. Cheng, "Dual-band differential phase shifter using phase-slope alignment on coupled resonators," *IEEE Microw. Wireless Compon. Lett.*, vol. 28, no. 12, pp. 1092–1094, Dec. 2018.
[72] Q. Dong, Y. Wu, W. Chen, Y. Yang, and W. Wang, "Single-layer dual-band bandwidth-enhanced filtering phase shifter with two different predetermined phase-shifting values," *IEEE Trans. Circuits Syst., II, Exp. Briefs*, vol. 68, no. 1, pp. 236–240, Jan. 2020.
[73] L.-L. Qiu and L. Zhu, "Synthesis design of dual-band differential phase shifters with independent filtering passbands and predetermined phase shifts," *IEEE Trans. Ind. Electron.*, vol. 69, no. 2, pp. 1791–1799, Feb. 2021.
[74] P.-L. Chi and T. Itoh, "Miniaturized dual-band directional couplers using composite right/left-handed transmission structures and their applications in beam pattern diversity systems," *IEEE Trans. Microw. Theory Techn.*, vol. 57, no. 5, pp. 1207–1215, May 2009.
[75] J. Vivos, T. Crepin, M.-F. Foulon, and J. Sokoloff, "Unbalanced metamaterials applied to phase shifter: Dedicated design method and application in C-band," *Prog. Electromagn. Res. C*, vol. 93, pp. 1–17, May 2019.
[76] N. A. Muhammad, S. K. A. Rahim, N. M. Jizat, T. A. Rahman, K. G. Tan, and A. W. Reza, "Beam forming networks using reduced size Butler matrix," *Wireless Pers. Commun.*, vol. 63, no. 4, pp. 765–784, Apr. 2012.
[77] T.-S. Horng, "A rigorous study of microstrip crossovers and their possible improvements," *IEEE Trans. Microw. Theory Techn.*, vol. 42, no. 9, pp. 1802–1806, Sep. 1994.
[78] W. Liu, Z. Zhang, Z. Feng, and M. Iskander, "A compact wideband microstrip crossover," *IEEE Microw. Wireless Compon. Lett.*, vol. 22, no. 5, pp. 254–256, May 2012.
[79] J.-J. Yao, C. Lee, and S.-P. Yeo, "Microstrip branch-line couplers for crossover application," *IEEE Trans. Microw. Theory Techn.*, vol. 59, no. 1, pp. 87–92, Jan. 2010.
[80] J. V. Tirado, E. Bernaola, and P. de Paco, "A compact microstrip crossover based on capacitively-loaded artificial transmission lines branch-line sections," *Prog. Electromagn. Res. Lett.*, vol. 68, pp. 121–126, Jun. 2017.
[81] D. A. Letavin, "Compact crossover based on low-pass filters," in *Proc. 19th Int. Conf. Young Spec. Micro/Nanotechnol. Electron Devices (EDM)*, Jun. 2018, pp. 192–194.
[82] V. M. Jayakrishnan and S. K. Menon, "Ring based planar crossover for beamforming networks," *Proc. Technol.*, vol. 25, pp. 629–634, Jan. 2016.
[83] V. M. Jayakrishnan and K. M. Sreedevi, "Circular microstrip patch assisted planar crossover for GPS application," in *Proc. Prog. Electromagn. Res. Symp. Spring (PIERS)*, 2017, pp. 2995–2999.
[84] M. A. B. Abbasi, M. A. Antoniades, and S. Nikolaou, "A compact microstrip crossover using NRI-TL metamaterial lines," *Microw. Opt. Technol. Lett.*, vol. 60, no. 11, pp. 2839–2843, Nov. 2018.
[85] R. Sinha and A. De, "Comments on 'design of a microstrip dual-band crossover with asymmetrical Π-shaped transmission lines,'" *IEEE Microw. Wireless Compon. Lett.*, vol. 26, no. 7, pp. 496–497, Jul. 2016.
[86] C.-W. Tang, K.-C. Lin, and W.-M. Chuang, "Design of a microstrip dual-band crossover with asymmetrical Π-shaped transmission lines," *IEEE Microw. Wireless Compon. Lett.*, vol. 25, no. 9, pp. 588–590, Sep. 2015.
[87] I. S. Krishna, R. K. Barik, and S. S. Karthikeyan, "Analysis and design of a planar crossover for dual-frequency applications," in *Proc. 14th IEEE India Council Int. Conf. (INDICON)*, Dec. 2017, pp. 1–5.
[88] Y. Cui and H. Hayashi, "Miniaturized microstrip dual-band branch-line crossover with two inner open stubs," *Prog. Electromagn. Res. Lett.*, vol. 82, pp. 59–64, Mar. 2019.
[89] S. Menon, "Microstrip patch antenna assisted compact dual band planar crossover," *Electronics*, vol. 6, no. 4, p. 74, Sep. 2017.
[90] M. Bayat, H. Shahi, and J. Mazloum, "Dual-band balanced-to-single-ended crossover based on composite right- and left-handed transmission lines," *Electron. Lett.*, vol. 56, no. 8, pp. 380–382, Apr. 2020.
[91] R. Garg, I. Bahl, and M. Bozzi, *Microstrip Lines and Slotlines*. Norwood, MA, USA: Artech House, 2013.
[92] H. A. Wheeler, "Transmission-line properties of a strip on a dielectric sheet on a plane," *IEEE Trans. Microw. Theory Techn.*, vol. MTT-25, no. 8, pp. 631–647, Aug. 1977.
[93] D. Hernandez, Y. Han, S. Son, and K.-N. Kim, "Design of microstrip transmission line array for magnetic resonance imaging at 300 MHz for spinal cord examination," *J. Electromagn. Waves Appl.*, vol. 35, no. 9, pp. 1125–1139, Jun. 2021.
[94] S. Z. Ibrahim, M. K. A. Rahim, T. Masri, M. N. A. Karim, and M. Z. A. A. Aziz, "Multibeam antenna array with Butler matrix for WLAN applications," in *Proc. 2nd Eur. Conf. Antennas Propag. (EuCAP)*, 2007, pp. 1–5.
[95] A. Shastrakar and U. Sutar, "Design and simulation of microstrip Butler matrix elements operating at 2.4 GHz for wireless applications," *Int. J. Sci.*, vol. 7, no. 5, pp. 1528–1531, May 2016.
[96] Y.-J. Kim, Y.-B. Kim, H.-J. Dong, Y. S. Cho, and H. L. Lee, "Compact switched-beam array antenna with a Butler matrix and a folded ground structure," *Electronics*, vol. 9, no. 1, p. 2, Dec. 2019.
[97] Z. Mousavi and P. Rezaei, "Millimetre-wave beam-steering array antenna by emphasising on improvement of Butler matrix features," *IET Microw., Antennas Propag.*, vol. 13, no. 9, pp. 1287–1292, Jul. 2019.
[98] G. A. Adamidis, I. O. Vardiambasis, M. P. Ioannidou, and T. N. Kapetanakis, "Design and implementation of single-layer 4 × 4 and 8 × 8 Butler matrices for multibeam antenna arrays," *Int. J. Antennas Propag.*, vol. 2019, pp. 1–12, Mar. 2019.
[99] C. Dall'Omo, T. Monediere, B. Jecko, F. Lamour, I. Wolk, and M. Elkael, "Design and realization of a 4 × 4 microstrip Butler matrix without any crossing in millimeter waves," *Microw. Opt. Technol. Lett.*, vol. 38, no. 6, pp. 462–465, 2003.
[100] P. Bhowmik and T. Moyra, "Modelling and validation of a compact planar Butler matrix by removing crossover," *Wireless Pers. Commun.*, vol. 95, no. 4, pp. 5121–5132, Aug. 2017.
[101] A. M. Zaidi, B. K. Kanaujia, and M. T. Beg, "A novel design of single band 4 × 4 Butler matrix using branch line couplers without a crossover and a phase shifter," in *Proc. Antennas Design Meas. Int. Conf. (ADMInC)*, Oct. 2019, pp. 130–134.
[102] K. Han, W. Li, and Y. Liu, "Flexible phase difference of 4 × 4 Butler matrix without phase-shifters and crossovers," *Int. J. Antennas Propag.*, vol. 2019, pp. 1–7, Dec. 2019.
[103] S. A. Babale, S. K. A. Rahim, O. A. Barro, M. Himdi, and M. Khalily, "Single layered 4 × 4 Butler matrix without phase-shifters and crossovers," *IEEE Access*, vol. 6, pp. 77289–77298, 2018.
[104] J. M. Wen, C. K. Wang, W. Hong, Y. M. Pan, and S. Y. Zheng, "A wideband switched-beam antenna array fed by compact single-layer Butler matrix," *IEEE Trans. Antennas Propag.*, vol. 69, no. 8, pp. 5130–5135, Aug. 2021.
[105] O. A. Safia, M. Nedil, M. C. E. Yagoub, and W. Yusuf, "Optically transparent compact 4 × 4 Butler matrix for Wi-Fi applications," *Prog. Electromagn. Res. Lett.*, vol. 58, pp. 119–124, Jan. 2016.
[106] P. H. Rao, J. S. Sajin, and K. Kudesia, "Miniaturisation of switched beam array antenna using phase delay properties of CSRR-loaded transmission line," *IET Microw., Antennas Propag.*, vol. 12, no. 12, pp. 1960–1966, Oct. 2018.

[107] F. Pizarro, D. Ramírez-Gil, A. Algaba-Brazález, L. F. Herrán-Ontanón, and E. Rajo-Iglesias, "Comparison study of 4 × 4 Butler matrices in microstrip technologies for Ka-band," *AEU - Int. J. Electron. Commun.*, vol. 122, Jul. 2020, Art. no. 153248.

[108] R. Karimian, M. D. Ardakani, S. Ahmadi, and M. Zaghloul, "High resolution beam switch antenna based on modified CRLH Butler matrix," *Eng. Rep.*, vol. 3, no. 1, Jan. 2021, Art. no. e12287.

[109] N. Ashraf, A.-R. Sebak, and A. A. Kishk, "PMC packaged single-substrate 4 × 4 Butler matrix and double-ridge gap waveguide horn antenna array for multibeam applications," *IEEE Trans. Microw. Theory Techn.*, vol. 69, no. 1, pp. 248–261, Jan. 2020.

[110] N. Ashraf, A. A. Kishk, and A.-R. Sebak, "AMC packaged–Butler matrix for millimeter wave beamforming," in *Proc. IEEE Int. Symp. Antennas Propag. USNC/URSI Nat. Radio Sci. Meeting*, Jul. 2018, pp. 417–418.

[111] S. I. Naqvi, M. A. Azam, Y. Amin, J. Loo, and H. Tenhunen, "Beam-steerable antenna array with metasurface at millimeter wave frequency range," in *Proc. 22nd Int. Multitopic Conf. (INMIC)*, 2019, pp. 1–6.

[112] A. K. Vallappil, M. K. A. Rahim, B. A. Khawaja, and M. N. Iqbal, "Compact metamaterial based 4 × 4 Butler matrix with improved bandwidth for 5G applications," *IEEE Access*, vol. 8, pp. 13573–13583, 2020.

[113] M. Du and H. Peng, "Ultra-compact electromagnetic metamaterial transmission line and its application in miniaturized Butler matrix," *Prog. Electromagn. Res. C*, vol. 55, pp. 187–197, 2014.

[114] C.-W. Wang, T.-G. Ma, and C.-F. Yang, "A new planar artificial transmission line and its applications to a miniaturized Butler matrix," *IEEE Trans. Microw. Theory Techn.*, vol. 55, no. 12, pp. 2792–2801, Dec. 2007.

[115] D. A. Letavin, "Microstrip matrix Butler area which is reduced by the use of compact directional couplers," in *Proc. 23rd Int. Conf. Appl. Electromagn. Commun. (ICECOM)*, Sep. 2019, pp. 1–3.

[116] D. A. Letavin, "Planar Butler matrix based on compact taps," in *Proc. IEEE East-West Design Test Symp. (EWDTS)*, Sep. 2019, pp. 1–3.

[117] D. C. Ravshanov, D. A. Letavin, and I. A. Terebov, "Butler matrix 4 × 4 ultra high frequency," in *Proc. Syst. Signal Synchronization, Generating Process. Telecommun. (SYNCHROINFO)*, Jul. 2020, pp. 1–4.

[118] P. K. Deb, T. Moyra, and B. K. Bhattacharyya, "Designing of miniaturized 4 × 4 Butler matrix using coupled line coupler and Schiffman phase shifter," *Iranian J. Sci. Technol., Trans. Electr. Eng.*, vol. 45, no. 1, pp. 259–268, Mar. 2021.

[119] C. Collado, A. Grau, and F. De Flaviis, "Dual-band Butler matrix for WLAN systems," in *IEEE MTT-S Int. Microw. Symp. Dig.*, Jun. 2005, pp. 2247–2250.

[120] N. Jizat, S. K. A. Rahim, M. Z. M. Nor, Y. Abdulrahman, M. I. Sabran, and M. F. Jamlos, "Beamforming network using dual band-dual beam reduced size Butler matrices," *Radioengineering*, vol. 22, no. 3, p. 769, 2013.

[121] K. Wincza, K. Staszek, I. Slomian, and S. Gruszczynski, "Scalable multibeam antenna arrays fed by dual-band modified Butler matrices," *IEEE Trans. Antennas Propag.*, vol. 64, no. 4, pp. 1287–1297, Apr. 2016.

[122] S. Zhou, Y. Liu, and Y. Wu, "Dual-band Butler matrix with the same phase difference for long-term evolution applications," *Electromagnetics*, vol. 36, no. 1, pp. 55–65, Jan. 2016.

[123] A. M. Zaidi, S. A. Imam, B. K. Kanaujia, K. Rambabu, K. Srivastava, and M. T. Beg, "A new dual band 4 × 4 Butler matrix with dual band 3 dB quadrature branch line coupler and dual band 45° phase shifter," *AEU Int. J. Electron. Commun.*, vol. 99, pp. 215–225, Feb. 2019.

[124] A. M. Zaidi, M. T. Beg, B. K. Kanaujia, J. Kishor, and K. Rambabu, "A novel dual band branch line coupler and its application to design a dual band 4 × 4 Butler matrix," *IEEE Access*, vol. 8, pp. 65104–65115, 2020.

[125] D. Deslandes and K. Wu, "Integrated microstrip and rectangular waveguide in planar form," *IEEE Microw. Wireless Compon. Lett.*, vol. 11, no. 2, pp. 68–70, Feb. 2001.

[126] T. Paul, M. Harinath, S. K. Garg, S. Aich, A. Kumar, J. Trivedi, A. Kumar, M. K. Patel, C. V. N. Rao, and R. Jyoti, "Miniaturized high-power beam steering network using novel nonplanar waveguide Butler matrix," *IEEE Microw. Wireless Compon. Lett.*, vol. 31, no. 6, pp. 678–681, Jun. 2021.

[127] K. Wu, D. Deslandes, and Y. Cassivi, "The substrate integrated circuits—A new concept for high-frequency electronics and optoelectronics," in *Proc. 6th Int. Conf. Telecommun. Modern Satell., Cable Broadcast. Service, (TELSIKS)*, 2003, pp. 1–8.

[128] K. Wu, M. Bozzi, and N. J. G. Fonseca, "Substrate integrated transmission lines: Review and applications," *IEEE J. Microw.*, vol. 1, no. 1, pp. 345–363, Jan. 2021.

[129] T. Djerafi, N. J. G. Fonseca, and K. Wu, "Design and implementation of a planar 4 × 4 Butler matrix in SIW technology for wide band high power applications," *Prog. Electromagn. Res. B*, vol. 35, pp. 29–51, 2011.

[130] Q.-L. Yang, Y.-L. Ban, K. Kang, C.-Y.-D. Sim, and G. Wu, "SIW multi-beam array for 5G mobile devices," *IEEE Access*, vol. 4, pp. 2788–2796, 2016.

[131] N. Tiwari and T. R. Rao, "A switched beam antenna array with Butler matrix network using substrate integrated waveguide technology for 60 GHz wireless communications," *AEU-Int. J. Electron. Commun.*, vol. 70, no. 6, pp. 850–856, Jun. 2016.

[132] S. Dey, N. S. Kiran, and S. Dey, "SIW Butler matrix driven beam scanning array for millimeter wave 5G communication," in *Proc. IEEE Asia–Pacific Microw. Conf. (APMC)*, Dec. 2020, pp. 709–711.

[133] M. M. Pezhman, A.-A. Heidari, and A. Ghafoorzadeh-Yazdi, "A compact 4 × 4 SIW beamforming network for 5G applications," *AEU Int. J. Electron. Commun.*, vol. 135, Jun. 2021, Art. no. 153714.

[134] S. Karamzadeh, V. Rafii, M. Kartal, and B. S. Virdee, "Compact and broadband 4 × 4 SIW Butler matrix with phase and magnitude error reduction," *IEEE Microw. Wireless Compon. Lett.*, vol. 25, no. 12, pp. 772–774, 2015.

[135] L.-H. Zhong, Y.-L. Ban, J.-W. Lian, Q.-L. Yang, J. Guo, and Z.-F. Yu, "Miniaturized SIW multibeam antenna array fed by dual-layer 8 × 8 Butler matrix," *IEEE Antennas Wireless Propag. Lett.*, vol. 16, pp. 3018–3021, 2017.

[136] Q. Sun, Y.-L. Ban, Y.-X. Che, and Z. Nie, "Coexistence-mode CRLH SIW transmission line and its application for longitudinal miniaturized Butler matrix and multibeam array antenna," *IEEE Trans. Antennas Propag.*, vol. 69, no. 11, pp. 7593–7603, Nov. 2021.

[137] C. Qin, F.-C. Chen, and K.-R. Xiang, "A 5 × 8 Butler matrix based on substrate integrated waveguide technology for millimeter-wave multi-beam application," *IEEE Antennas Wireless Propag. Lett.*, vol. 20, no. 7, pp. 1292–1296, Jul. 2021.

[138] E. T. Der, T. R. Jones, and M. Daneshmand, "Miniaturized 4 × 4 Butler matrix and tunable phase shifter using ridged half-mode substrate integrated waveguide," *IEEE Trans. Microw. Theory Techn.*, vol. 68, no. 8, pp. 3379–3388, May 2020.

[139] R. Lu, C. Yu, Y. Zhu, and W. Hong, "Compact millimeter-wave end-fire dual-polarized antenna array for low-cost multibeam applications," *IEEE Antennas Wireless Propag. Lett.*, vol. 19, no. 12, pp. 2526–2530, Dec. 2020.

[140] Q. Sun, Y.-L. Ban, J.-W. Lian, Y. Liu, and Z. Nie, "Millimeter-wave multibeam antenna based on folded C-type SIW," *IEEE Trans. Antennas Propag.*, vol. 68, no. 5, pp. 3465–3476, May 2020.

[141] M. M. M. Ali and A.-R. Sebak, "2-D scanning magnetoelectric dipole antenna array fed by RGW Butler matrix," *IEEE Trans. Antennas Propag.*, vol. 66, no. 11, pp. 6313–6321, Nov. 2018.

[142] I. Afifi and A.-R. Sebak, "Wideband 4 × 4 Butler matrix in the printed ridge gap waveguide technology for millimeter-wave applications," *IEEE Trans. Antennas Propag.*, vol. 68, no. 11, pp. 7670–7675, Mar. 2020.

[143] P.-S. Kildal, E. Alfonso, A. Valero-Nogueira, and E. Rajo-Iglesias, "Local metamaterial-based waveguides in gaps between parallel metal plates," *IEEE Antennas Wireless Propag. Lett.*, vol. 8, pp. 84–87, 2008.

[144] A. Berenguer, V. Fusco, D. E. Zelenchuk, D. Sánchez-Escuderos, M. Baquero-Escudero, and V. E. Boria-Esbert, "Propagation characteristics of groove gap waveguide below and above cutoff," *IEEE Trans. Microw. Theory Techn.*, vol. 64, no. 1, pp. 27–36, Jan. 2015.

[145] E. Rajo-Iglesias, M. Ferrando-Rocher, and A. U. Zaman, "Gap waveguide technology for millimeter-wave antenna systems," *IEEE Commun. Mag.*, vol. 56, no. 7, pp. 14–20, Jul. 2018.

[146] A. Algaba-Brazalez and E. Rajo-Iglesias, "Design of a Butler matrix at 60 GHz in inverted microstrip gap waveguide technology," in *Proc. IEEE Int. Symp. Antennas Propag. USNC/URSI Nat. Radio Sci. Meeting*, Jul. 2015, pp. 2125–2126.

[147] F. J. G. Bernal and E. Rajo-Iglesias, "Design of a wide band Butler matrix in groove gap waveguide technology," in *Proc. Int. Symp. Antennas Propag. (ISAP)*, Oct. 2017, pp. 1–2.

[148] L.-Q. Luo, L. Chen, and Y.-F. Yang, "A ridge gap waveguide 4 × 4 Butler matrix for multibeam application," in *Proc. Cross Strait Radio Sci. Wireless Technol. Conf. (CSRSWTC)*, Oct. 2021, pp. 410–412.

[149] D. Zarifi, A. Farahbakhsh, and A. U. Zaman, "A 60 GHz-band 4 × 4 Butler matrix based on ridge gap waveguide," in *Proc. 16th Eur. Conf. Antennas Propag. (EuCAP)*, Mar. 2022, pp. 1–3.

[150] C. Wang, Y. Yao, X. Cheng, Z. Zhu, and X. Li, "A W-band high-efficiency multibeam circularly polarized antenna array fed by GGW Butler matrix," *IEEE Antennas Wireless Propag. Lett.*, vol. 20, no. 7, pp. 1130–1134, Jul. 2021.

[151] J. Cao, H. Wang, S. Tao, S. Mou, and Y. Guo, "Highly integrated beam scanning groove gap waveguide leaky wave antenna array," *IEEE Trans. Antennas Propag.*, vol. 69, no. 8, pp. 5112–5117, Aug. 2021.
[152] A. Tamayo-Domínguez, J. Fernández-González, and M. Sierra-Castañer, "3-D-printed modified Butler matrix based on gap waveguide at W-band for monopulse radar," *IEEE Trans. Microw. Theory Techn.*, vol. 68, no. 3, pp. 926–938, Mar. 2019.
[153] C. Caloz and T. Itoh, "Novel microwave devices and structures based on the transmission line approach of meta-materials," in *IEEE MTT-S Int. Microw. Symp. Dig.*, vol. 1, Jun. 2003, pp. 195–198.

ABDULKADIR BELLO SHALLAH (Member, IEEE) was born in Gwandu, Kebbi, Nigeria, in 1984. He received the B.Eng. degree in electrical and electronics engineering from Bayero University, Kano, in 2014, and the M.Eng. degree in electronics and telecommunications from Universiti Teknologi Malaysia, in 2017, where he is currently pursuing the Ph.D. degree with the School of Electrical Engineering.

He has been a Lecturer with the Electrical and Electronics Engineering Department, Faculty of Engineering, Kebbi State University of Science and Technology, Aliero, Kebbi. His research interests include RF and microwave devices, reflectarray antennas, beamforming networks, and metamaterials.

FARID ZUBIR (Member, IEEE) received the B.Eng. degree in electrical (majoring in telecommunication) and the M.Eng. degree in RF and microwave from Universiti Teknologi Malaysia (UTM), in 2008 and 2010, respectively, and the Ph.D. degree from the University of Birmingham, U.K., in 2016, for research into direct integration of power amplifiers with antennas in microwave transmitters. He currently serves as an Assistant Professor with the Department of Communication Engineering, School of Electrical Engineering, UTM. In 2019, he secured the scholarship to work as an Honorary Postdoctoral Research Fellow for a period of two years at The University of British Columbia (UBCO), Okanagan, BC, Canada, where he was conducting research into highly efficient and linear amplification power amplifier topology for wireless power systems. His research interests and specialization include the area of RF and microwave technologies, including linearization and high-efficiency techniques for PAs, planar array antenna, dielectric resonator antenna (DRA), and active integrated antenna (AIA).

MOHAMAD KAMAL A. RAHIM (Senior Member, IEEE) was born in Alor Setar, Malaysia, in 1964. He received the B.Eng. degree in electrical and electronic engineering from the University of Strathclyde, U.K., in 1987, the master's degree in engineering from the University of New South Wales, Australia, in 1992, and the Ph.D. degree in wideband active antenna from the University of Birmingham, U.K., in 2003. From 1992 to 1999, he was a Lecturer with the Faculty of Electrical Engineering, Universiti Teknologi Malaysia, where he was a Senior Lecturer with the Department of Communication Engineering, from 2005 to 2007 and is currently a Professor. His research interests include the design of active and passive antennas, dielectric resonator antennas, microstrip antennas, reflectarray antennas, electromagnetic bandgap, artificial magnetic conductors, left-handed metamaterials, and computer-aided design for antennas.

HUDA A. MAJID (Member, IEEE) received the Ph.D. degree in electrical engineering from Universiti Teknologi Malaysia (UTM). He worked as a Postdoctoral Fellow with UTM for a period of one year. He is currently a Senior Lecturer with the Faculty Engineering Technology, Universiti Tun Hussein Onn Malaysia (UTHM), Batu Pahat, Johor. He has published over 100 papers in journals and conferences. His research interests include planar and flexible antennas, array antennas, reconfigurable antennas, metamaterial, and RF microwave and mm-wave devices.

USMAN ULLAH SHEIKH (Senior Member, IEEE) received the Ph.D. degree in image processing and computer vision from Universiti Teknologi Malaysia, in 2009. He is currently a Senior Lecturer with the Department of Computer and Electrical Engineering, Faculty of Engineering, Universiti Teknologi Malaysia. His research interests include computer vision, machine learning, and embedded systems design.

NOOR ASNIZA MURAD (Senior Member, IEEE) received the B.E. degree in electrical and telecommunications engineering, and the M.E. degree in electrical engineering from Universiti Teknologi Malaysia (UTM), in 2001 and 2003, respectively, and the Ph.D. degree from the Emerging Device Technology Group, University of Birmingham, U.K., in 2011, for research on micromachined millimeterwave circuits. Shortly after graduation, she served UTM as a Tutor with the Department of Radio Communication Engineering (RaCED), Faculty of Electrical Engineering (FKE), UTM, where she was appointed as a Lecturer, in April 2003. She is currently an MBOT Professional Technologist and an Associate Professor with the School of Electrical Engineering, UTM. She attached to HID GLOBAL Sdn Bhd, for one year, under research and development specifically working on RFID tag design, testing, and development. Her research interests include antenna design for RF and microwave communication systems, millimeterwave circuits design, RFID, and antenna beamforming.

ZUBAIDA YUSOFF (Senior Member, IEEE) received the B.Sc. degree *(cum laude)* in electrical and computer engineering and the M.Sc. degree in electrical engineering from The Ohio State University, USA, in 2000 and 2002, respectively, and the Ph.D. degree from Cardiff University, Wales, U.K., in 2012. She worked with Telekom Malaysia International Network Operation, in 2002, before she joined Multimedia University, Malaysia, in 2004, where she currently holds the position of a Senior Lecturer at the Faculty of Engineering. She has authored/co-authored more than 50 journals and conference papers. Her teaching and research focus in the area of power amplifier design, antenna, 5G communications, and analog/mixed signal RF circuit design. She has presented technical papers at conference nationally and internationally. One of her conference papers has received the "Honorable Mention" for the Student Paper Competition at the International Microwave Symposium, USA, in 2011.